OF 2004-4

Open File

New Nouveau
Brunswick

Natural Resources
Minerals, Policy and Planning

SOUTHERN NEW BRUNSWICK POTENTIAL FIELDS PROJECT, PART III: GRAVITY AND MAGNETIC METHODS APPLIED TO GRANITE-RELATED MINERAL EXPLORATION IN CHARLOTTE COUNTY, NEW BRUNSWICK

M.S. King and S.M. Barr

ISSN 1702-2649
ISBN 1-55396-336-9
Price: $15.00

2004

Open File 2004-4

Southern New Brunswick Potential Fields Project, Part III: Gravity and Magnetic Methods Applied to Granite-related Mineral Exploration in Charlotte County, New Brunswick

Recommended citation:

KING, M.S. and BARR, S.M. 2004. Southern New Brunswick potential fields project, Part III: Gravity and magnetic methods applied to granite-related mineral exploration in Charlotte County, New Brunswick. New Brunswick Department of Natural Resources; Minerals, Policy and Planning Division, Open File 2004-4, 76 p.

Prepared for:

Minerals, Policy and Planning Division
Department of Natural Resources
Province of New Brunswick

Hon. Keith Ashfield
Minister of Natural Resources

May, 2004

104-07316/

New Nouveau
Brunswick

Natural Resources
Minerals, Policy and Planning

Open File 2004-4

Southern New Brunswick Potential Fields Project, Part III: Gravity and Magnetic Methods Applied to Granite-related Mineral Exploration in Charlotte County, New Brunswick

M.S. King[1] and **S.M. Barr**[2]

[1] Consulting Geophysicist, Halifax, Nova Scotia
[2] Acadia University, Wolfville, Nova Scotia

ISSN 1702-2649
ISBN 1-55396-336-9
Price: $15.00

2004

Table of Contents

LIST OF FIGURES II

LIST OF TABLES II

ABSTRACT III

1.0 INTRODUCTION 1

1.1 PROJECT SCOPE 1
1.2 PROJECT OBJECTIVES 2
1.3 PREVIOUS WORK 3
1.4 GEOLOGICAL BACKGROUND 4

2.0 GRAVITY DATA 6

2.1 DESCRIPTION 6
2.2 PROCESSING AND ENHANCEMENT 7

3.0 MAGNETIC DATA 7

3.1 DESCRIPTION 7
3.1 PROCESSING AND ENHANCEMENT 8

4.0 DIGITAL ELEVATION DATA 9

4.1 DESCRIPTION 9

5.0 PETROPHYSICAL DATA 9

5.1 DESCRIPTION 9

6.0 POTENTIAL FIELD MODELS 11

6.1 BACKGROUND 11
6.2 DESCRIPTION 12

7.0 MAP PATTERN INTERPRETATION 12

7.1 MAGNETIC DATA 12
7.2 BOUGUER GRAVITY DATA 14

8.0 POTENTIAL FIELD MODEL INTERPRETATION 15

9.0 DISCUSSION 20

10.0 CONCLUSIONS AND RECOMMENDATIONS 26

11.0 REFERENCES 29

12.0 FIGURE CAPTIONS AND FIGURES 1-12 34

APPENDIX I: GRAVITY SURVEY SPECIFICATIONS AND DIGITAL DATA . 49

APPENDIX II: POTENTIAL FIELD MODEL DESCRIPTIONS AND MODELS (LEGEND AND LINES 1-10) 63

List of Figures

Figure 1.	Project location map with 1:50000 geology base map.	37
Figure 2.	Project location map with compiled gravity stations and regional geology.	38
Figure 3.	Colour contoured (1 mGal) residual Bouguer gravity and regional geology.	39
Figure 4.	Colour contoured / shaded relief magnetic total field image and regional geology.	40
Figure 5.	Colour contoured / shaded relief calculated second vertical derivative image and regional geology.	41
Figure 6.	Colour contoured / shaded relief calculated horizontal derivative (east-west) image and regional geology.	42
Figure 7.	Colour contoured / shaded relief calculated horizontal derivative (north-south) image and regional geology.	43
Figure 8.	Calculated digital elevation model (DEM) and regional geology.	44
Figure 9.	Project area with 2003 sample locations and regional geology.	45
Figure 10.	Project area with model locations and regional geology.	46
Figure 11.	Magnetic lineament analysis and regional geology.	47
Figure 12.	Colour contoured depth to G1 and G2 with summary interpretations and regional geology.	48

List of Tables

Table 1.	List of intrusions and age data.	5
Table 2.	Summary of physical property data.	10

Abstract

Several significant granite-related mineral occurrences (e.g. Clarence Stream and Mount Pleasant) are located north of the Magaguadavic Granite in a regional gravity low coarsely delineated by existing gravity surveys. A new program was designed to collect high-quality gravity data to more accurately delineate this gravity feature and individual anomalies associated with isolated plutons in the area. Physical property data were generated from a sample suite consisting of host rocks (from outcrop) in the Mascarene and St. Croix terranes and many of the intrusions in the study area (from outcrop and drill core) in order to augment potential field interpretations. Utilizing the new geophysical data, as well as magnetic and digital elevation data recently acquired in a high-resolution aeromagnetic survey completed by the Geological survey of Canada, a three-dimensional interpretation was made that focused on the geometry and distribution of granitoid bodies.

The results of the study indicate that the Clarence Stream gold occurrences are situated in an area transected by a major northwest-trending fault system that can be mapped using magnetic data. Based on potential field modeling, the area north of the Magaguadavic Granite, including the Clarence Stream gold occurrences, is underlain by a felsic body (G2) with low density and low magnetic susceptibility that intruded the area after the main phase (DM1) of the Magaguadavic granite was emplaced and cooled. The G2 body has geophysical characteristics similar to those of the John Lee Brook Granite to the east. Younger (ca. 360 Ma) intrusions associated with the main Sn-W-Mo polymetallic deposits in the area intrude G2 in the eastern part of the study area. Geophysical map patterns, supported by three-dimensional modeling interpretations, infer that these small bodies may be part of a more continuous intrusive system related to the Mount Pleasant Porphyry and/or the McDougall Brook microgranite. The shapes and relationships of these intrusions to one another have been refined by the geophysical data. Gold mineralization in this area has been interpreted on the basis of other studies to be related to fluids emanating from the Magaguadavic Granite along faults trending northeast. However, these data do not preclude the involvement of the G2 intrusion in

gold mineralization, or the potentially significant role played by the northwest-trending fault systems defined by this geophysical study.

Résumé

Plusieurs venues minérales granitiques importantes (p. ex. ruisseau Clarence et mont Pleasant) sont situées au nord du granite de Magaguadavic dans un creux gravimétrique régional grossièrement délimité par les levés gravimétriques existants. Un nouveau programme visait à recueillir des données gravimétriques de première qualité pour délimiter de façon plus exacte cette particularité gravimétrique et chacune des anomalies associées au pluton isolé du secteur. On a obtenu des données sur les propriétés physiques d'un cortège échantillon constitué de roches hôtes (d'un affleurement) des terranes de Mascarene et de St. Croix ainsi que d'un grand nombre d'intrusions dans le secteur d'étude (de l'affleurement et de carottes de sondage) afin d'enrichir les interprétations du champ de potentiel. Les chercheurs ont utilisé les nouvelles données géophysiques ainsi que des données altimétriques numériques et magnétiques récemment tirées d'un levé aéromagnétique à haute résolution réalisé par la Commission géologique du Canada pour effectuer une interprétation tridimensionnelle axée sur la géométrie et la répartition des masses granitiques.

Les résultats de l'étude révèlent que les venues aurifères du ruisseau Clarence sont situées dans un secteur coupé transversalement par un système de failles important orienté vers le nord-ouest pouvant être cartographié au moyen de données magnétiques. Selon la modélisation du champ de potentiel, le secteur au nord du granite de Magaguadavic, y compris les venues aurifères du ruisseau Clarence, repose sur une masse felsique (G2) de faible densité et de faible susceptibilité magnétique ayant pénétré dans le secteur après la mise en place et le refroidissement de la phase principale (DM1) du granite de Magaguadavic. La masse G2 possède des caractéristiques géophysiques analogues à celles du granite du ruisseau John Lee à l'est. Les intrusions plus récentes (environ 360 Ma) associées aux principaux gîtes polymétalliques de Sn-W-Mo du secteur pénètrent dans G2 dans la partie orientale du secteur d'étude. Les configurations cartographiques géophysiques, appuyées par les interprétations de modélisation

tridimensionnelle, laissent supposer que ces petites masses pourraient faire partie d'un système intrusif plus continu apparenté au porphyre du mont Pleasant ou au microgranite du ruisseau McDougall. Les chercheurs ont précisé les formes de ces intrusions et leurs rapports les unes avec les autres au moyen des données géophysiques. Ils ont, en s'appuyant sur d'autres études, interprété la minéralisation aurifère dans ce secteur comme une minéralisation apparentée à des fluides provenant du granite de Magaguadavic le long de failles orientées vers le nord-est. Ces données n'écartent toutefois pas la possibilité de la participation de l'intrusion G2 à la minéralisation aurifère ni d'un rôle possiblement déterminant des systèmes de failles orientés vers le nord-ouest définis par cette étude géophysique.

1.0 Introduction

This project was conducted under the auspices of a collective research agreement between the New Brunswick Department of Natural Resources and Energy and Acadia University (principle investigator Sandra M. Barr). It forms part of an ongoing geological research programme in southern New Brunswick by the second author.

1.1 Project Scope

In previous work, King and Barr (2003b, 2003c) proposed that the Clarence Stream gold deposit is underlain by and possibly related to a low-density granite that post-dates the Magaguadavic Granite (i.e. <396 Ma). The authors postulated a relationship between the younger intrusion and the satellite plutons collectively referred to as the "Pomeroy intrusive suite" by McLeod (1990); however, the interpretation was based on one potential field model constructed using regional-quality (i.e. +/- 1 mGal) gravity points, and no physical property information was available from these intrusions to assist in the testing of the model. Hence, the present project was developed to acquire high-quality (+/- 0.2 mGal) gravity data over an area defined by a significant regional gravity low (~40-45 mGal) that includes the satellite plutons ("Pomeroy intrusive suite") north of the Magaguadavic Granite (Fig. 1), and to generate a representative physical property database from outcrop and drill core samples to support magnetic and gravity data interpretation.

Gravity data were collected over previously mapped intrusions (e.g. Magaguadavic Granite, Tower Hill Granite, Pleasant Ridge Granite, Beech Hill Pluton, McDougall Brook Microgranite and Kedron Pluton) in a systematic regional grid pattern

from which interdependent 2¾-D models were constructed to assess the three-dimensional geometry and relationships between intrusions in the study area. Petrophysical properties, including magnetic susceptibility and density data, were used to discriminate between intrusions of different lithologies and ages. These data were compared to geometric relationships derived from the potential field models to assess the emplacement history of the intrusions in the study area. Furthermore, several structural and stratigraphic relationships were assessed in light of known mineral occurrences and regional geochemical trends. The results of the project are presented here.

1.2 Project Objectives

This part of the Southern New Brunswick Potential Fields Project was intended to build upon previous regional data and interpretations to develop a more detailed, applied procedure to compliment regional and detailed exploration strategies for granite-related mineralization. In particular, the goals of this program were to utilize a combination of gravity, magnetic, petrophysical, and digital elevation data to:

a) Identify previously unmapped shallow intrusions.

b) More accurately delineate the subsurface distribution (i.e. three-dimensional) of newly defined and previously mapped intrusions.

c) Discriminate between intrusions of different compositions and/or ages.

d) Identify regional structures and/or stratigraphic units related to known mineral occurrences or mineralizing systems.

e) Combine results of (a) through (d) to develop a regional exploration concept.

1.3 Previous Work

With the exception of work by the present authors (King and Barr 2002b, c), detailed interpretations of regional geophysical data in the project area have not been published. Prior to the acquisition of high-resolution aeromagnetic data in the area, Thomas and Willis (1989) used regional quality gravity data and a limited database of density values to model the Saint George Batholith. They assumed a uniform density of 2.60 g/cm^3 for all units comprising the batholith, including satellite plutons of the "Pomeroy intrusive suite" (McLeod 1990). Thomas and Willis (1989) constructed a gravity model across several of the satellite intrusions (i.e. Sorrell Ridge and Pleasant Ridge) north of the Magaguadavic Granite (Fig. 10; p. 574). They concluded that the undivided Saint George Batholith (density 2.60 g/cm^3) underlies the entire area and suggested that the Sorrel Ridge, Pleasant Ridge, and Beech Hill intrusions are extensions of the batholith.

King and Barr (2003b) used newly acquired gravity data and high-resolution aeromagnetic data to model a section approximately coincident with a portion of line 1 of Thomas and Willis (1989) (Fig 6.; p. 570). New geophysical information, in particular magnetic data, and a more detailed understanding of pre-Carboniferous basement (e.g. King 2002; King and Barr 2003a) allowed subdivision of the Saint George Batholith into a magnetic, moderate density unit (i.e. Magaguadavic Granite) and a non-magnetic, slightly lower density unit tentatively associated with the satellite plutons comprising the Pomeroy intrusive suite. King and Barr (2003b) interpreted this intrusion to be younger than the Magaguadavic Granite based on geometric relationships derived from the potential field model. They suggested that the younger intrusion might be related to post-

orogenic extension and a series of faults trending northwest-southeast. Using northwest-trending breaks in the magnetic signature, assumed to be related to magmatic layering in the Magaguadavic Granite, they suggested that fluids related to this younger, lower density intrusion could have played a role in forming the gold mineralization at the Clarence Stream deposit.

1.4 Geological Background

The project area is underlain by units associated with the Ordovician St. Croix terrane and the Silurian Mascarene terrane (Fyffe 1997; McLeod et al. 1998). The Mascarene Group of the Mascarene terrane represents a cover sequence over the New River and St. Croix terranes (Fyffe and Fricker 1987; Fyffe et al. 1999). It consists of a variety of formations, but in the project area, the Mascarene Group is represented by the Waweig Formation, dominated by sedimentary and volcaniclastic rocks. The St. Croix terrane in the project area is comprised of sedimentary rocks from the Cookson Group, including the Calais and Kendall Mountain formations. The Sawyer Brook Fault, a regional-scale east-northeast trending, dextral late-D_3 structure (e.g., Castonguay et al. 2003), separates units of the Mascarene and St. Croix terranes. These terranes were amalgamated by the latest Silurian and intruded by numerous Late Silurian, Devonian, and Late Devonian plutons comprising the Saint George Batholith (McLeod 1990; McLeod et al. 1994), which dominates the southern two-thirds of the study area. McLeod (1990) and others have documented a temporal evolution from mafic-felsic units (i.e. Welsford Complex, Bocabec Gabbro, and Utopia Granite) to felsic units (i.e. John Lee Brook and Mount Douglas granites) with distinct associations to gold, base-metal, and granophile-element mineralization.

Several significant granite-related mineral occurrences have been documented (e.g. McLeod et al. 1994a) in the project area. Most notable are the porphyry-hosted Mount Pleasant polymetallic deposit and the Clarence Stream gold deposit (Fig. 1). Numerous authors (e.g. Thorne and Lentz 2001; Castonguay et al. 2002; Thorne et al. 2002; Watters and Castonguay 2002) have investigated the structural constraints and geochemical signature of the Clarence Stream gold deposit and concluded that the deposit is structurally controlled, and that veining associated with the gold mineralization is genetically related to the Magaguadavic Granite. Thorne and McLeod (2003) also discussed several other mineral occurrences related to Devonian intrusions including the Kedron (tin-gold), McDougall Brook (gold), and Tower Hill (gold) occurrences.

Accurate age data for the various intrusions in the project area are lacking, as only the Magaguadavic and Mount Douglas units have been dated using U-Pb analysis (Table 1). Other intrusions in the area are either undated, or have been dated using $^{40}Ar/^{39}Ar$ or Rb-Sr methods with uncertain reliability or significance.

Table 1. Summary of age data from intrusions.

Intrusion Name	Age (Ma)	Dating Method	Reference
Mount Pleasant Porphyry	ca 360	$^{40}Ar/^{39}Ar$	Sinclair et al. 1988
Pleasant Ridge Granite	ca 361	$^{40}Ar/^{39}Ar$	Taylor (1992)
Kedron Pluton	ca 362	$^{40}Ar/^{39}Ar$	Taylor (1992)
Mount Douglas Granite	ca 367	U-Pb and $^{40}Ar/^{39}Ar$	Bevier (1988, 1990) McLeod (1988, 1990)
John Lee Brook Granite	ca 384	$^{40}Ar/^{39}Ar$	McLeod et al. (1990)
Magaguadavic Granite	ca 396	U-Pb and $^{40}Ar/^{39}Ar$	Bevier (1990) McLeod (1990)
Tower Hill Granite	ca 401	Rb-Sr	Whalen et al. (1994)

Thorne et al. (2002) studied the petrology, geochemistry, and geochronology of granitic dykes associated with gold mineralization at the Clarence Stream deposit. They presented data from the Magaguadavic Granite (DM_1 and DM_2), John Lee Brook Granite, and True Hill, Pleasant Ridge and Sorrel Ridge plutons. Thorne et al. (2002) concluded that the gold mineralization at the Clarence Stream deposit is temporally and genetically related to late fractionated units (DM_2) of the Magaguadavic Granite, despite some geochemical similarities to other units, including the John Lee Brook Granite and younger units that comprise the Pomeroy intrusive suite of McLeod (1990).

Castonguay et al. (2002, 2003) investigated the regional structural geology in the Clarence Stream and Moores Mills areas and found that several gold occurrences, including the Clarence Stream gold deposit, are hosted by northeast-trending brittle-ductile fault zones and/or dilatant zones related to late F_2 and F_3 folds. They suggested that regional structures and lithology (to the degree where competent units are more likely to generate dilatant zones) likely played a major role in concentrating gold mineralization in these occurrences, as has been documented in intrusion-related deposits in other gold districts (e.g. Thompson and Newberry 2000).

2.0 Gravity Data

2.1 Description

King and Barr (2003b, c) completed a compilation of existing gravity data and acquired 84 new stations in 2002 in the present study area. Together these data represent 326 stations with variable quality regional-type (i.e. +/- 1 mGal accuracy) gravity measurements for an average of 1 station per 3.85 km^2 (project area = 1256 km^2).

The present study included the acquisition of an additional 426 high quality (+/- 0.2 mGal) gravity points (Appendix I), thereby increasing gravity coverage in the study area to 1 station per 1.63 km^2. Data were collected over known intrusions primarily along roads crossing regional trends. Several longitudinal or tie line surveys were also completed in order to level cross-sections to one another, thus providing additional constraints on geological models derived from the modeling process. The new gravity survey (Fig 2.) provides stand-alone high quality gravity coverage for a large portion of the study area; however, for regional interpretations the new data were merged with existing data to provide maximum coverage.

2.2 Processing and Enhancement

The Bouguer gravity data were merged and gridded using a 200 m cell size. Gravity profile data for the potential field models were extracted from a residual of the 200 m grid (Fig. 3). The residual grid was derived by the removal of a first order regional polynomial trend from the original total field data; more details on this procedure can be found in King and Barr (2003b) and Telford et al. (1988).

3.0 Magnetic Data

3.1 Description

Fugro Sial Airborne Surveys Incorporated completed the St. Stephen aeromagnetic survey (#304) in 2001 on behalf of the Geological Survey of Canada (GSC). Fugro used a fixed wing platform to acquire high-resolution magnetic data between October 21 and December 12. The sensor height was 100 m and flight lines were

spaced 200 m apart. Survey lines were oriented 144°/324° and a total of 26,800 km, including control lines, were acquired. Real time differential navigational data (i.e. UTM X, UTM Y, altitude) that were collected during the survey were processed by the contractor and a coincident set of ground elevation data points were generated. The leveled magnetic total field and elevation data were archived and provided to the authors in digital ASCII XYZ format using the UTM NAD27 (Zone 20) coordinate system.

3.1 Processing and Enhancement

The magnetic total field data for the project area were gridded using a 50 m cell size (Fig. 4) and vertical and horizontal gradients were derived from this gridded data. The second vertical derivative (Fig. 5) of the measured total field data was calculated to enhance very shallow features, generally less than 500 m deep, at the expense of deeper geological sources. These data provided enhanced resolution from which structural and stratigraphic map patterns were interpreted.

Horizontal derivatives were calculated from the total magnetic field data in the east-west (Fig. 6) and north-south (Fig. 7) directions. These data were used to highlight lateral changes in magnetic character related to lithological variations and/or major structural breaks.

A residual magnetic grid was also calculated for the purpose of extracting measured profiles for use in the potential field models using a procedure similar to that used on the gravity data (Section 2.1). Regional-residual separation of the magnetic data set removed trends related to variations in the earth's magnetic field.

4.0 Digital Elevation Data

4.1 Description

Elevation models frequently provide a useful base for potential field data and aid in the interpretation of map patterns. Elevation data were also extracted for use in the potential field models and were derived from a spatially continuous source similar to the magnetic and gravity grids.

The digital elevation model (DEM) was constructed by gridding the elevation data, generated during the airborne survey (Section 3.1), using a 50 m cell size (Fig. 8). A check of the airborne DEM versus the elevation control from the 2003 gravity survey (Section 2.0) produced an RMS error of 2.76 m (N=446). It is noted that this error could manifest itself as a change in the amplitude of short wavelength anomalies in the calculated (not measured) gravity profile. However, the scale of the models constructed for this report rendered this effect negligible.

5.0 Petrophysical Data

5.1 Description

Specific gravity (i.e. density) and magnetic susceptibility measurements were made on 304 samples collected from outcrop (n=182), sub-crop (n=2) and drill core (n=120) in the study area (Fig. 9). Petrophysical determinations were made under laboratory conditions using procedures documented by King (2002) and the sample suite included most major units and intrusions in the study area. The data are summarized in

Table 2, and include mean and standard deviation values that were calculated for each map unit using a simple statistics component from a commercial spreadsheet package.

Table 2. Summary of physical property measurements from units in the study area. Magnetic susceptibility (Susc.) units are $x10^{-3}$ SI; Density units are g/cm^3; n = number of samples. * Values estimated from potential field models. New River unit values are from King and Barr (2003b); where numbers differ, n refers to susceptibility and density measurements, respectively.

Name	Lithology	n	Susc.	+/-	Density	+/-
Calais Formation	sedimentary/volcanic	7	0.27	0.08	2.75	0.03
Digdeguash Formation	sedimentary	43	0.29	0.10	2.75	0.07
East Branch Brook Gabbro	gabbro	7	0.79	0.51	2.94	0.05
Flume Ridge Formation	sedimentary	17	0.18	0.07	2.70	0.04
John Lee Brook Granite	granite	4	0.14	0.22	2.61	0.02
Kedron Pluton (BR84-2, 4)	granite	11	0.12	0.05	2.74	0.09
Kedron Pluton (BR84-2; peg.)	granite	5	0.8	0.98	2.65	0.02
Kedron Pluton (BR84-3)	granite	8	0.09	0.01	2.62	0.01
Kendall Mountain Formation	sedimentary	49	0.35	0.37	2.72	0.05
Magaguadavic Granite	granite	10	13.09	3.63	2.65	0.02
McDougall Brook Microgranite	granite	6	0.65	0.84	2.59	0.01
Pleasant Ridge Granite	granite	11	0.08	0.01	2.67	0.01
Sand Brook Formation	sedimentary	2	0.38	0.04	2.87	0.06
Sorrel Ridge Granite	granite	19	0.18	0.1	2.64	0.03
Tower Hill Granite	granite	22	0.13	0.03	2.69	0.02
True Hill Granite	granite	44	0.22	0.17	2.65	0.06
Utopia Granite	granite	4	0.07	0.22	2.60	0.01
Waweig Formation	sedimentary/volcanic	35	0.59	0.62	2.75	0.09
Granite Intrusion (G1)	granite	n/a	1.00*	n/a	2.63*	n/a
Granite Intrusion (G2)	granite	n/a	0.10*	n/a	2.61*	n/a
New River Belt volcanic units	volcanic rocks	5/3	6.88	7.08	2.70	0.03
Leavitts Head volcanic unit	rhyolite	3/3	4.35	5.06	2.68	0.02
Ragged Falls Pluton	gabbro, granite, syenogranite	24/22	2.48	3.10	2.72	0.12

6.0 Potential Field Models

6.1 Background

Potential field models were constructed using data (i.e. observed) extracted from the DEM, residual magnetic, and residual gravity grids. Geological control was derived from the 1:50 000 scale maps produced by the New Brunswick Department of Natural Resources and Energy (e.g. Fyffe 1997; Fyffe et al. 1998; McLeod et al. 1997; Fyffe et al. 1998). Map units in the Mascarene and St. Croix terrane were subdivided primarily on the basis of magnetic response; however, associated physical properties correspond to the data shown in Table 2. The geological models are left undivided at depth or where little or no geological control is present; physical properties for these undivided components were derived from an average value of the overlying or nearest units in each particular terrane. As such, undivided units do not have any particular geological significance. The basement component for all models in this report has physical properties most characteristic of the Gander terrane (e.g. King and Barr 2003a, c). King and Barr (2003a, c) provided a detailed discussion on the relevance of this geophysical basement.

Computational parameters included appropriate values for the Bouguer density, geomagnetic field, elevation, and topography. Most of the bodies comprising the geological models are designated as 2¾-D in that they have limited and variable strike in and out of the section (e.g. King and Barr 2003c). All bodies are oriented at 90° strike to the section.

6.2 Description

Ten sections were selected to investigate the subsurface geometry and relationships between mapped intrusions, including those inferred from gravity map patterns (Fig. 10). Because this project was designed primarily to investigate granite-related mineralization, it was most useful to select lines with orientations at large angles to mapped or inferred granite bodies, as opposed to overlying (magnetic) stratigraphy. Three models were constructed from longitudinal profiles (regional strike ~070°) and seven cross-section models were constructed (Appendix II). The relatively uniform geometry of the intrusions and comparatively lower sensitivity of gravity data to strike facilitated the fit of measured to calculated gravity profiles (<0.2 mGal RMS). However, the magnetic data are quite sensitive to strike and hence considerable variability between the calculated and measured profiles resulted from changes of orientation along strike. For instance, the three longitudinal lines have portions essentially parallel to strike and other portions at oblique angles and still other portions at nearly right angles. As only one value for the strike of the geological models can be used per line it was impossible to fit most magnetic units. The abundance of intrusions and complicated geometry also caused some discrepancies between calculated and measured profiles.

7.0 Map Pattern Interpretation

7.1 Magnetic Data

The magnetic total field map (Fig. 4) is dominated by the positive response associated with the Magaguadavic Granite (Ma). Internally, this response is interpreted to reflect magnetic layering, which is in turn affected by younger crosscutting structures.

Other high amplitude positive magnetic features are associated with the Bocabec Gabbro and McDougall Brook Microgranite (MB); however, the Mount Pleasant Porphyry associated with the Mount Pleasant deposit ("C" Fig. 4) is characterized by a low magnetic response similar to that of the adjacent John Lee Brook Granite. The Tower Hill (TH) Granite is coincident with a distinct magnetic low and the Pleasant Ridge (PR) Granite and Kedron (Ke) plutons are located in a subtle, but distinct, northeast-trending positive magnetic feature. The Sorrel Ridge Granite (SR) shows little magnetic response and in fact local stratigraphic trends imaged in the magnetic data appear undisturbed by the intrusion, suggesting that the Sorrel Ridge Granite consists of little more than dykes, at least in the near surface.

Numerous distinct magnetic anomalies form a series of northwest-trending linear features cutting the concentric magnetic anomaly patterns that are most likely associated with magmatic layering in the Magaguadavic Granite. These features are characterized by linear magnetic lows (Fig. 5) and in several instances they can be related to mapped faults. Outside of the Magaguadavic Granite, they can be traced to breaks in magneto-stratigraphy (e.g. Kendall Mountain Formation) but, in places, subtle positive anomalies are also evident. Several examples occur due east of the Kedron Pluton (Ke).

The northwest-trending faults defined by mapping and herein by magnetic patterns also offset some major east-west trending structures. One such major east-west structure cuts the southern third of the Magaguadavic Granite and results in a dramatic change of magnetic character. The total field (Fig. 4) and vertical derivative (Fig. 5) data give little indication of the significance of this feature but the horizontal derivative data (Fig. 7) provide clear evidence for a large amount of vertical displacement. This

qualitative interpretation was assessed in three dimensions with potential field models 8 and 9.

A documentation of northwest-trending magnetic lineaments in the study area (Fig. 11) shows a concentration of features through an east-northeast trend along the northern contact of the Magaguadavic Granite and the area immediately to the north.

7.2 Bouguer Gravity Data

Residual Bouguer gravity data (Fig. 3) generally correlate well with mapped boundaries of intrusions in the study area, with the exception of the Magaguadavic Granite. The fact that gravity map patterns show little direct correlation with the margins of the Magaguadavic Granite suggests that the pluton has limited depth extent and/or that dramatic lithological changes occur at relatively shallow depths.

Gravity patterns can be generally divided into three trends oriented at roughly 060-080°. The first trend (north) occurs along the northern third of the study area and originates in the Moores Mills area west of the Tower Hill Granite (TH). It may extend east as far as the McDougall Brook pluton. Gravity values in this trend are comparatively high with respect to the other trends. The lowest gravity values in the survey area are in the central trend and include isolated anomalies coincident with satellite plutons (e.g. SR, PR and Ke) north of the Magaguadavic Granite. The eastern portion of the central trend appears to be interrupted by a series of northwest-trending structures, including a major dextral northwest-trending fault that forms the western contact of the John Lee Brook Granite with the Magaguadavic Granite. This portion of the central trend contains the Beech Hill (BH) and True Hill (Tr) granites and the Mount Pleasant Porphyry, and includes the Mount Pleasant deposit ("C", Fig. 3). The third residual Bouguer gravity

trend (south trend) is a low that underlies the John Lee Brook Granite and strikes west-southwest to the "Main Zone" area of the Clarence Stream gold occurrences ("B", Fig. 3). The central and south anomalies merge toward the eastern part of the study area.

The new Bouguer gravity data and associated processing have provided new insight particularly in regards to buried intrusions and relationships between intrusions, both mapped and buried. Some examples include the large anomaly surrounding the relatively small Tower Hill Granite (TH) and a small distinct gravity lobe extending from the Sorrel Ridge Granite anomaly. This latter feature strikes to the southwest beneath Whittier Ridge and correlates with a pronounced topographic feature (Fig. 8). Other relationships include the Kedron Pluton (Ke) linked as a satellite to the Pleasant Ridge Granite and local trends that include the Beech Hill – True Hill – Mount Pleasant intrusions.

8.0 Potential Field Model Interpretation

Geological models derived from potential field data were constrained by new petrophysical measurements and correlate well with geological information in the project area. These models demonstrate that significant changes in the geometry and relationships of the intrusions to one another occur at relatively shallow depths. Furthermore, geometrical relationships inferred from the geological models suggest a relative timing of intrusive events, which is consistent with present age information. The geometry of the intrusions is discussed from oldest to youngest as inferred by intrusive relationships derived from geological models (Appendix II):

a) Tower Hill Granite (TH) - is a steep-sided, depth-limited body. The central unit (DTHfib; Fyffe, 1997) overlies the deepest portion (2200-2500 m) of the intrusion

whereas the southern lobe extends only to a depth of approximately 1000 m. The northern lobe appears to be a thin veneer underlain by younger granite (i.e. G1).

b) Magaguadavic Granite (Ma) – is a broad intrusion with complex subsurface geometry. The southern third has been cut by a significant regional fault, trending east-west, that has resulted in several thousand metres of vertical displacement (south side up). This fault was recognized in the magnetic horizontal gradient data (Fig. 7) and is modeled to coincide with the New River – St. Croix terrane boundary. The Magaguadavic Granite has a maximum depth of 7000-8000 m in the central part of the northern lobe and thins to 3000-4000 m at the northern contact. The northern contact of the Magaguadavic Granite is relatively steep; however, in all the geological models a small lobe protrudes several hundred metres north of the mapped contact. The Sawyer Brook Fault (Mascarene (MT) - St. Croix (SC) terrane boundary at surface) cuts the Magaguadavic Granite and displaces the north side up several hundred meters. The Magaguadavic Granite is intruded by two younger, possibly related, granite bodies (John Lee Brook granite and G2).

c) John Lee Brook Granite (JLB) – intrudes the Magaguadavic Granite, extends to a depth of more than 8000 m and has physical properties virtually identical to granite G2 (Table 2).

d) New Intrusion (G1 granite) – is younger than the Tower Hill Granite and coincides with the northern gravity trend discussed in Section 7.2. This intrusion underlies the Moores Mills-Tower Hill areas and is roughly coincident with a positive topographic feature in those areas. G1 appears to continue at depth to the

northeast for approximately 5-7 km and has an overall maximum depth of 9000-10000 m.

e) New Intrusion (G2 granite) – appears to intrude G1 and therefore is presumed to be younger. G2 is a low density and low magnetic susceptibility body (Table 2) with physical properties most similar to those of the John Lee Brook Granite. It occurs directly north of the Magaguadavic Granite and is bounded at depth to the west by G1 and appears to be intruded in the east by the McDougall Brook Microgranite and/or the Mount Pleasant Porphyry. The area directly above G2 is coincident with the highest frequency of northwest-trending magnetic linear trends discussed in Section 7.1. Hence, these anomalies appear to be directly related to the G2 intrusion and possibly to its associated fluid system.

f) Sorrel Ridge Granite (SR) – occurs as a small cupola directly related to G2. The Sorrel Ridge Granite has physical properties similar to those of G2, with slightly higher density and magnetic susceptibility values that are perhaps indicative of a larger amount of country rock assimilation. It appears from the geological models and map patterns that the Sorrel Ridge Granite is unrelated to the Pleasant Ridge and Beech Hill intrusions, unless the differences in geophysical properties are the result of variations produced during the evolution of intrusions derived from the same source.

g) Pleasant Ridge Granite (PR) – intrudes G1 and extends to a depth of 2000-3000 m. Line 1 contains the southernmost portion of the Pleasant Ridge Granite and from there it strikes northeast cutting line 3 (Appendix II) at an oblique angle.

h) Kedron Pluton (Ke) – appears to be an extension of the Pleasant Ridge Granite (e.g. Line 10; Appendix II). The Kedron Granite represents the extreme eastern part of the Pleasant Ridge system; however; it is possible that this system was once connected with the Beech Hill-True Hill system and was offset to the north along the McDougall Lake fault. This interpretation assumes a protracted movement history with several episodes of re-activation. Some indication of the sense and magnitude of fault may be seen in the offset of the Mascarene - St. Croix terrane boundary (e.g. Sawyer Brook Fault) on either side of the John Lee Brook Granite (Fig. 1).

i) Beech Hill (BH) – True Hill (Tr) granite bodies – intrude G2 and appear to be associated with the McDougall Brook Microgranite and the Mount Pleasant Porphyry based on spatial relationships and map patterns. This group of plutons occurs within a discrete gravity trend, and corresponding geological models show that the Beech Hill – True Hill system extends to depths of 2000 m (Line 2; Appendix II) to 1500 m (Line 3; Appendix II).

j) McDougall Brook Microgranite (MB)- intrudes G2; however, its relationship to the Beech Hill – True Hill system is equivocal. Magnetic map patterns (Fig. 4) suggest that the McDougall Brook Microgranite, as mapped (McLeod et al. 1994), might include a nonmagnetic unit modeled here on line 2. This unit could be associated with the Mount Pleasant porphyry.

The central portion of the study area is underlain by a granite intrusion (G2) at a depth of 1000 to 2000 m (Fig. 12). Based on the shape of the body derived from geophysical modeling, intrusion G2 was emplaced after the main portion (DM_1) of the

Magaguadavic Granite. Also based on shapes defined by modeling, younger plutons (360 Ma?) appear to have intruded the G2 granite and correlate with discrete positive relief features in the DEM (Fig. 8).

St. Croix terrane units appear to be dipping fairly steeply and in some cases (e.g. line 1) appear to contain repeated stratigraphy as defined by density and magnetic susceptibility values. It is worth noting that there are certain limitations to the spatial relationships between some of the host units in the geological models because of similar or overlapping physical property values (Table 2; King and Barr 2003b). The first example deals with the upper and lower Saint Croix terrane units. The lower units (SC-u) are undivided because small-scale variations in magnetic susceptibility between units at these depths, like those that occur in near surface units, would generate only subtle anomalies that are difficult to image in geophysical data. These anomalies are overshadowed by higher amplitude, shorter wavelength anomalies caused by near-surface (e.g. <2000 m depth) units (SC). Physical property values for the lower units were derived from the average values of the overlying units. This boundary is not intended to represent any physical contact; more so it is the limit to which geometric interpretations (i.e. contact dips) can be interpreted from short wavelength magnetic anomalies.

The second example involves units comprising the Saint Croix (SC) and Mascarene (MT) terranes, which have similar physical properties. As such there is little broad geophysical contrast across the boundary between these two terranes, delineated at surface by the northeast-trending Sawyer Brook Fault. However, in most cases the geometry of magnetic anomalies in the terranes immediately adjacent to the Sawyer Brook Fault define a sub-vertical fabric and as such the Sawyer Brook Fault must also be

a steeply dipping structure. In addition, the general orientation of the contacts between bodies comprising the St. Croix and Mascarene terranes in the geological models (Appendix II), as defined by the shape of isolated magnetic anomalies, is north-dipping in the Saint Croix terrane and south-dipping in the Mascarene terrane. The boundary between these two steeply dipping magnetic fabrics is coincident with the approximate location of the Sawyer Brook Fault.

The third example relates to the true thickness of the Mascarene (MT) terrane where it overlies Saint Croix terrane rocks. Because at the bulk or "terrane level" these two terranes have similar physical properties, they are geophysically difficult to distinguish when oriented in a horizontal setting.

Finally, units beneath the Magaguadavic Granite (Ma) labeled NR (New River terrane) and SC (Saint Croix terrane) on lines 8 and 9 (Appendix II) are largely unconstrained by geological mapping. However, the units comprising the New River terrane south of lines 8 and 9 are distinctly more magnetic than exposed units comprising the Saint Croix and Mascarene terrane in these areas (Table 2). This magnetic contrast is incorporated into the geological models, resulting in the present interpretation (see also King and Barr 2003c).

9.0 Discussion

This study combined previously available high-resolution magnetic and archived gravity data with newly acquired high-quality gravity data to assess map patterns over granite intrusions associated with known mineral deposits (e.g. Clarence Stream and Mount Pleasant) in Charlotte County, southern New Brunswick. Potential field modeling utilized these new data, as well as petrophysical measurements, to construct a three-

dimensional geological model for these intrusions. A digital elevation model (DEM) was derived, and several distinct relief patterns correlate precisely with mapped intrusions and potential field map patterns. These data showed that several systematic features are associated with granite-related mineralization in the study area.

Magnetic map patterns associated with the Magaguadavic Granite provide a temporal reference for several concepts developed during the course of this study. Probable magmatic layering is defined by a series of concentric magnetic anomalies coincident with the main body (DM_1, north lobe) of the Magaguadavic Granite (396 Ma; U-Pb, Bevier, 1990). These magnetic patterns are in turn cut by two generations of regional structures, an older set trending east-west and a younger set trending northwest-southeast. Based on geological models (lines 8 and 9; Appendix II), at least one major east-west trending structure cuts the Magaguadavic Granite and displaces the southern third of the granite up several thousand meters relative to the northern part. This major structure is in turn cut by a series of dextral(?) northwest-trending structures, presumably related to the Devonian Acadian orogeny and reactivated during post-orogenic extension and later Carboniferous events. These structures display distinct magnetic signatures (low or negative anomalies) and occur with greatest frequency in or just to the north of the Magaguadavic Granite. The low or negative magnetic anomalies, interpreted to result from alteration of magnetite-rich layers in the Magaguadavic Granite, provide direct evidence of these structures, whereas outside of the granite indirect evidence is provided by offsets or breaks in magnetic patterns that are likely caused by pyrrhotite-rich layers in volcanic and sedimentary units of the St. Croix terrane. The alteration indicated by the low or negative magnetic anomalies associated with these structures indicates that they

may have been conduits for hydrothermal fluids from an event which post-dated emplacement and cooling of the Magaguadavic Granite. We suggest that these fluids may have been generated during the emplacement of intrusion G2 and younger granite plutons. These intrusions may have locally reactivated overlying structures, which would explain the higher frequency of northwest-trending magnetic anomalies at or just to the north of the northern margin of the Magaguadavic Granite.

The role of these northwest-trending structures in the present distribution of mineralization at the Clarence Stream gold deposit is uncertain. These structures occur in the ore zones (e.g. the AD Zone; Thorne and McLeod 2003, Fig. 3, p. 53) and likely offset NE-trending ore zones (Watters et al. 2003). Gold showings and soil anomalies defined by Freewest Resources Canada Inc. occur along a northwest trend directly coincident with one of the northwest-trending structural features shown by the magnetic data extending through the Magaguadavic Granite (Fig. 6). The magnetic pattern suggests that this structure is comprised of at least two parallel faults. Geochemical data collected by Freewest Resources Canada Inc. also show two parallel gold-in-soil anomalies that form a linear pattern approximately 500-700 m wide and more than 2000 m long. These geochemical patterns are consistent with either a broad northwest-trending source or a series of point sources aligned along a northwest trend. They could also be caused by overlapping sources along a northeasterly trend enhanced by glacial dispersion along a topographic feature, as dispersion trails of this magnitude are common in the region (e.g. Balzer 1992). However, the DEM does not reveal any lineaments in the area of the geochemical anomalies that would suggest a glacial/topographic control, although in such DEM lineaments are present locally elsewhere in the study area (Fig. 8).

Exploration and mapping programs in the Clarence Stream area have indicated that significant emphasis should be placed on the Sawyer Brook Fault and other unnamed northeast-trending structures in constraining mineralized zones (M. McLeod, pers. comm. 2003). The geophysical data of this study suggest that significant mineralized zones may be located at the intersection of northwest-trending and northeast-trending structures. These intersections may have formed larger spaces where mineralizing or re-mobilizing fluids migrating along northeast- and northwest-trending large-scale faults, might accumulate. Such fluids may have been related to the previously unrecognized intrusion G2 which underlies the area.

The gravity signature associated with the Magaguadavic Granite is inconsistent with mapped boundaries and physical property data, in that the southern part is underlain by a relative gravity high, and the gravity low beneath the northern lobe extends well beyond the mapped margin of the pluton into the St. Croix terrane. Analysis of map patterns and geological models derived from potential field models indicates that the relative gravity high in the south is the result of a major regional fault. The gravity low in the north is interpreted to be the result of the presence of a younger and less dense intrusion. This body, referred to as G2 has to have low magnetic susceptibility and density compared to the Magauadavic Granite in order to generate the measured potential field response (e.g. Fig. 4). The values required (2.61 g/cm^3 and 0.10 x10^{-3} SI) unequivocally distinguish G2 from the Magaguadavic Granite (2.65 g/cm^3 and 13.1 x10^{-3} SI) and also from several other intrusions in the area.

Potential field models define the location of G2 to be just north of the Magaguadavic Granite, bounded at depth to the east by the Mount Pleasant Porphyry

and/or McDougall Brook Microgranite and to the west by another previously unmapped intrusion, referred to here as G1. The area above G2 is directly coincident with the highest frequency of northwest-trending magnetic anomalies discussed above; hence, this body is interpreted to have locally reactivated northwest-trending (and possibly northeast-trending) structures. This intrusion may also have been the source of fluids that altered primary magnetite to produce magnetic lows along the northwest-trending structures and may also have been involved in producing gold mineralization in the Clarence Stream area. We suggest that this previously unrecognized G2 intrusion may have played a critical role in generating gold mineralization in the Clarence Stream area.

The relationship between intrusions G2 and G1 is equivocal; however, some spatial relationships in the geological models suggest that G2 intruded G1, although it is possible that the two intrusions are coeval. The geological models (Appendix II) suggest that G1 is younger than the Tower Hill Granite and G2 is younger than the Magaguadavic Granite. Physical property data and the geological models indicate that the Sorrel Ridge Granite is distinct from the Pleasant Ridge, Beech Hill and Mount Pleasant group of intrusions. The Sorrel Ridge Granite is modeled as a cupola directly related to G2 whereas the Pleasant Ridge and Beech Hill plutons intrude G2 (e.g. line 2; Appendix II), and hence are younger. The Kedron Pluton appears to represent the extreme eastern part of the Pleasant Ridge pluton, and the Beech Hill intrusion includes the True Hill plutons. It is possible that these plutons were once part of a more continuous intrusion connected to the Mount Pleasant Porphyry. Northwest-trending regional faults, including the McDougall Lake fault, may offset the Pleasant Ridge intrusive package from the Beech

Hill intrusive package. The latter occurs within a distinct magnetic and gravity trend, which contains the Mount Pleasant polymetallic deposit.

Historical drilling for Mount Pleasant-style mineralization in the area focused on the periphery of satellite plutons, spatial extents of which were not clearly defined by outcrop control. The new gravity data presented in this report redefine the shape and distribution of many of these intrusions and identify possible new intrusions. These data are supported by a digital elevation model (DEM) which has features directly correlated to mapped plutons and postulated subsurface plutons. The DEM correlates spatially to intrusions but also appears to differentiate on the basis of relative relief (i.e. negative versus positive) between older, more mafic (Magaguadavic Granite) and younger more felsic (G2, G1, Sorrel Ridge, Pleasant Ridge, Beech Hill, McDougall Brook Microgranite and Mount Pleasant Porphyry) intrusions. The G1 intrusion could be the source for the large contact metamorphic aureole in the vicinity of the Tower Hill pluton. Quartz stockwork and sulfide mineralization were observed in this area during the 2003 gravity survey and the outline of the granite is roughly coincident with a broad positive topographic feature.

Potential field map patterns (Figs. 3 and 4) are not consistent with mapped unit boundaries in the Mount Pleasant area. Physical property data from samples collected during this project, as well as the geological models (e.g. line 2; Appendix II), indicate that the Mount Pleasant Porphyry may be distinguished from the McDougall Brook Microgranite on the basis of magnetic susceptibility and magnetic map patterns. Map patterns and interpretations (e.g. Fig. 11) suggest that the contact between the Mount Pleasant Porphyry and the McDougall Brook Microgranite to the north may be associated

with a major northwest-trending structure and that the non-magnetic Mount Pleasant Porphyry may underlie a larger area to the south of this feature.

10.0 Conclusions and Recommendations

This project was successful in demonstrating the utility of a multi-disciplinary approach toward using geophysical data in regional mineral exploration. Geophysical interpretations supported by physical property data provide reasonably explicit geological models. The 2003 field component demonstrated that sample collection and analysis, in addition to industry-quality gravity acquisition, are highly cost-effective exploration tools. Previous geological models were tested and new geological models proposed. The results of this project may have broad implications for base and precious metal exploration in southern New Brunswick. In particular, the definition of regional structures and mapping the distribution of younger intrusions (<396 Ma) contribute to an understanding of the physical role that they may play in mineralization.

This work has suggested that some correlations may exist between gold mineralization and northwest-trending structures locally reactivated by intrusions that post-date the Magaguadavic Granite (DM_1). Specifically, the recognition of a large previously unrecognized felsic intrusion G2 in the subsurface under the Clarence Stream gold occurrences suggests a genetic link with gold mineralization.

Geophysical evidence does not support the interpretation that the Sawyer Brook Fault represents a significant tectonic feature; however, the lack of evidence may be related to the physical property similarity between units cut by the fault. In all probability mineralizing fluids from underlying granite would migrate along proximal structures regardless of orientation, an interpretation for which there is ample evidence, particularly

in the enhanced magnetic data. The key exploration tools are the ability to map these buried intrusions and identify areas where mineralized fluids may have concentrated.

Various intrusions in the study area can be distinguished on the basis of their density and magnetic susceptibility properties; hence, they can be mapped by regional magnetic and gravity surveys. Regional structures can also be distinguished through re-processing and enhancement of magnetic data with parameters designed for specific areas (e.g. background magnetic character and orientation of local geology). Targets identified through these methods can be prospected and tested through focused geochemical surveys.

Previous exploration for Mount Pleasant-style mineralization targeted the periphery of satellite plutons (e.g. Pleasant Ridge), boundaries of which were not well defined. The new gravity data presented here provide fresh insight into the subsurface distribution of these younger intrusions and their relationships to one another and intrusions that host the Mount Pleasant mineral occurrences. Previous exploration results might be re-interpreted in light of this new information and previous exploration models could be re-tested. For example, data presented here suggest that the Mount Pleasant Porphyry may occur over a larger area and regional structures (e.g. northwest-trending faults) may play a role in the present distribution of associated exploration targets.

Several models put forth here could be tested with additional geological and physical property information. In particular, drill core from many of the intrusions is available in the core library in Sussex, New Brunswick. Detailed petrological studies and accurate ages would shed additional light on relationships among the various intrusions and compositional variations within each intrusion. The physical property database for

several intrusions (e.g. Magaguadavic Granite (DM_2), John Lee Brook Granite, Mount Pleasant Porphyry) should be expanded using available core and outcrop sampling. A more detailed physical property study in concert with the recommended petrographic study is needed to address some variations within and between drill holes sampled in this study.

More detailed gravity data could be acquired in several areas to further define some of the trends occurring in the new data set (e.g. Pleasant Ridge – Beech Hill – Mount Pleasant trends). This work should be part of an expansion of the study area to the east to include more of the Mount Pleasant area and to the south to include the Mount Douglas Granite. A study with a scope similar to this project in that area would shed light on mineral occurrences, in addition to augmenting the results presented here.

11.0 References

Balzer, S.A. 1992. Quaternary geology and dispersal patterns in the Canterbury area, New Brunswick. New Brunswick Department of Natural Resources and Energy, Mineral Resources, Open File 92-5, 192 p.

Bevier, M.L. 1990. Preliminary U-Pb geochronological results for igneous and metamorphic rocks, New Brunswick. *In* Project Summaries for 1989, Fourteenth Annual Review of Activities, (ed) S.A. Abbott. New Brunswick Department of Natural Resources and Energy Division, Information Circular 89-2 (second edition), 208-212.

Castonguay, S., Watters, S., and Ravenelle, J. 2002. Regional structural geology of the Clarence Stream area, southwestern New Brunswick and implications for gold exploration. *In* Carroll, B.M.W (ed), Abstracts, 2002 27th annual Review of Activities. New Brunswick Department of Natural Resources and Energy; Minerals, Policy and Planning Division, Information Circular 2002-1, p. 16.

Castonguay, S., Watters, S., and Ravenelle, J-F. 2003. Preliminary report on the structural geology of the Clarence Stream-Moores Mills area, southwestern New Brunswick: implications for gold exploration. Geological Survey of Canada, Current Research 2003-D2, 10 p.

Fyffe, L.R. 1997. Geology of the Rollingdam area (NTS 21 G/06), Charlotte County, New Brunswick. New Brunswick Department of Natural Resources and Energy, Minerals and Energy Division, Plate 97-31. Revised 2002.

Fyffe, L.R., and Fricker, A. 1987. Tectonostratigraphic terrane analysis of New Brunswick. Maritime Sediments and Atlantic Geology, **23**, 113-122.

Fyffe, L.R., McLeod, M.J., and Johnson, S.C. 1998. Bedrock geological compilation of the St. Stephen area (NTS 21 G/03), Charlotte County, New Brunswick. New Brunswick Department of Natural Resources and Energy, Minerals and Energy Division, Plate 98-24. Revised 2002.

Fyffe, L.R., Pickerill, R.K., Stringer, P. 1999. Stratigraphy, sedimentology and structure of the Oak Bay and Waweig formations, Mascarene Basin: implications for the paleotectonic evolution of southwestern New Brunswick. Atlantic Geology, **35**, 59-84.

King, M.S. 2002. The Mira – Bras d'Or terrane boundary in Cape Breton Island, Nova Scotia: Potential field and petrophysical investigations applied to tectonic analysis in the northern Appalachian orogen. Unpublished M.Sc. thesis, Acadia University, Wolfville, Nova Scotia, 190 p.

King, M.S. and Barr, S.M. 2003a. Potential field and petrophysical investigations applied to tectonic analysis in the northern Appalachian orogen. *In* Geological Society of America, 2003 Abstracts with programs, Northeastern Section, 35, No. 3, p. 18.

King, M.S. and Barr, S.M. 2003b. Southern New Brunswick Potential Fields Project Part I: Implications for Granite-related Gold Mineralization in the Clarence Stream Area. New Brunswick Department of Natural Resources and Energy, Open File 2003-6, 49 p.

King, M.S. and Barr, S.M. 2003c. Southern New Brunswick Potential Fields Project Part II: Implications for tectonic analysis. New Brunswick Department of Natural Resources and Energy, Open File 2003-7, 93 p.

McLeod, M.J., Taylor, R.P., and Lux, D.R. 1988. $^{40}Ar/^{39}Ar$ geochronology and Sn-W-Mo-bearing sheeted veins of the Mount Douglas Granite, southwestern New Brunswick. Canadian Mining and Metallurgical Bulletin, 81, No. 918, 70-77.

McLeod, M.J. 1990. Geology, geochemistry, and related mineral deposits of the Saint George Batholith; Charlotte, Queens, and Kings Counties, New Brunswick. New Brunswick Department of Natural Resources and Energy, Mineral Resources, Mineral Resource Report 5, 169 p.

McLeod, M.J., Johnson, S.C. and Ruitenberg, A.A. 1994a. Geological map of southwestern New Brunswick. New Brunswick Department of Natural Resources and Energy, Mineral Resources, Map NR-5.

McLeod, M.J., Johnson, S.C., and Ruitenberg, A.A. 1994b. Geological map of southwestern New Brunswick. New Brunswick Department of Natural Resources and Energy, Mineral Resources, Map NR-6.

McLeod, M.J., Johnson, S.C., and Fyffe, L.R. 1998. Bedrock geological compilation of the McDougall Lake area (NTS 21 G/07), Charlotte County, New Brunswick. New Brunswick Department of Natural Resources and Energy, Minerals and Energy Division. Plate 98-25. Revised 2002.

Sinclair, W.D., Kooiman, G.J.A., and Martin, D.A. 1988. Geological setting of granites and related tin deposits in the North Zone, Mount Pleasant, New Brunswick. *In* Current Research, Part B. Geological Survey of Canada, Paper 88-1B, 201-208.

Taylor, R.P. 1992. Petrological and geochemical characteristics of the Pleasant Ridge zinnewaldite-topaz granite, southern New Brunswick, and comparisons with other topaz-bearing felsic rocks. Canadian Mineralogist, **30**, 895-921.

Telford, W.M., Geldart, L.P., Sheriff, R.E., and Keys, D.A. 1988. Applied Geophysics, Cambridge University Press, Cambridge, U.K., 860 p.

Thomas, M. D. and Willis, C. 1989. Gravity Modelling of the Saint George Batholith and adjacent terrane within the Appalachian Orogen, southern New Brunswick. Canadian Journal of Earth Sciences, **26**, 561-576.

Thompson J.F.H. and Newberry, R.J. 2000. Gold deposits related to reduced granitic intrusions. *In* Gold in 2000. *Edited by* S. Hagemann and P. Brown. Reviews in Economic Geology, 13, p. 377-400.

Thorne, K.G. and Lentz, D.R. 2001. Geochemistry and petrogenesis of the East Branch Brook metagabbroic dykes in the Sawyer Brook fault zone, Clarence Stream gold prospect, southwestern New Brunswick. Atlantic Geology, **37**, 175-190.

Thorne, K., and McLeod, M. 2003. Gold deposits associated with felsic intrusions in southwestern New Brunswick – Field guidebook. New Brunswick Department of Natural Resources and Energy; Minerals, Policy and Planning Division, Open File 2003-4, 83 p.

Thorne, K.G., Lentz, D.R., Hall, D.C., and Yang, X. 2002. Petrology, geochemistry, and geochronology of the granite pegmatite and aplite dykes associated with the Clarence

Stream gold deposit, southwestern New Brunswick. Geological Survey of Canada, Current Research, 2002-E12, 13 p.

Watters, S. and Castonguay, S. 2002. New gold occurrences in the Clarence Stream area of Southern New Brunswick: Anomaly "A" – structure, alteration and vein paragenesis. *In* Carroll, B.M.W (ed), Abstracts, 2002 27th Annual Review of Activities. New Brunswick Department of Natural Resources and Energy; Minerals, Policy and Planning Division, Information Circular 2002-1, p. 71.

Watters, S. Castonguay, S., and McLeod, M. 2003. Preliminary report on new gold occurrences in the Clarence Stream area of southern New Brunswick: Anomaly "A" - distal deposits of an intrusion - related -gold system? Geological Survey of Canada, Open File 1779, 40 p.

Whalen, J.B., Jenner, G.A., Currie, K.L., Barr, S.M., Longstaffe, F.J., and Hegner, E. 1994. Geochemical and isotopic characteristics of granitoids of the Avalon Zone, southern New Brunswick: possible evidence for repeated delamination events. Journal of Geology, **102**, 269-282.

12.0 Figure Captions and Figures 1-12

Figure 1. General location map showing geology contacts (black) and faults (red) from 1:50000 geology base (Fyffe 1997; Fyffe et al. 1998; McLeod et al. 1998). Major mineral occurrences: A = Clarence Stream MW and AD zones, B = Clarence Stream Main Zone and C = Mount Pleasant mine. Intrusion abbreviations: TH = Tower Hill Granite, Ma = Magaguadavic Granite, EB = East Branch Brook Gabbro, BG = Bocabec Gabbro, JLB = John Lee Brook Granite, SR = Sorrel Ridge Granite, MB = McDougall Brook Granite, PR = Pleasant Ridge Granite, Ke = Kedron Pluton, BH = Beech Hill Granite, Tr = True Hill Pluton. Geological abbreviations: OW = Woodland Formation, OKM = Kendall Mountain Formation, SW = Waweig Formation, SSB = Sand Brook Formation, SDI = Digdeguash Formation, SM = Mohannes Granite, SFR = Flume Ridge Formation, DB = Bocabec Complex, DLM = Little Mount Pleasant Formation.

Figure 2. General location map showing project area with old gravity stations (green symbols) and new gravity stations (red stars). Refer to Figure 1 caption for abbreviations.

Figure 3. Colour contoured residual Bouguer gravity data. Contour interval is 1 mGal. Red fills represent higher values and blue fills represent lower values. Refer to Figure 1 caption for abbreviations.

Figure 4. Colour contoured / shaded relief residual magnetic total field image. Shading from the north at 35° above the horizon. Red fills represent higher values and blue fills represent lower values. Refer to Figure 1 caption for abbreviations.

Figure 5. Colour contoured / shaded relief enhanced calculated magnetic second vertical derivative image. Shading from the north at 35° above the horizon. Red fills represent higher values and blue fills represent lower values. Refer to Figure 1 caption for abbreviations.

Figure 6. Colour contoured / shaded relief calculated magnetic horizontal (east-west) derivative image. Shading from the southeast at 35° above the horizon. Red fills represent higher values and blue fills represent lower values. Refer to Figure 1 caption for abbreviations.

Figure 7. Colour contoured / shaded relief calculated magnetic horizontal (north-south) derivative image. Shading from the southwest at 35° above the horizon. Red fills represent higher values and blue fills represent lower values. Refer to Figure 1 caption for abbreviations.

Figure 8. Colour contoured / shaded relief calculated digital elevation model (DEM). Shading from the north at 35° above the horizon. Red fills represent higher elevations and blue fills represent lower elevations. Refer to Figure 1 caption for abbreviations.

Figure 9. General location map showing project area with sample locations. Sample locations are shown with an X and drill hole locations are shown with a red circle and cross. Refer to Figure 1 caption for abbreviations.

Figure 10. General location map showing location of potential field models. Models are oriented from west to east and south to north. Refer to Figure 1 caption for abbreviations.

Figure 11. General location map showing Magnetic lineament interpretations: green lines correspond to magmatic layering in the Magaguadavic Granite and pink lines refer to crosscutting structures. Major east-west structures are shown as thicker pink lines. Refer to Figure 1 caption for abbreviations.

Figure 12. General location map showing distribution of G1 and G2 granite bodies interpreted from models (colour contours) and map patterns (dashed line). Colour

contour intervals (250 m) are approximate depth to top. Major structural features discussed in text are shown as continuous red fault lines where CSFZ = Clarence Stream Fault Zone and MLFZ = McDougall Lake Fault Zone. Refer to text and Figure 1 caption for other abbreviations.

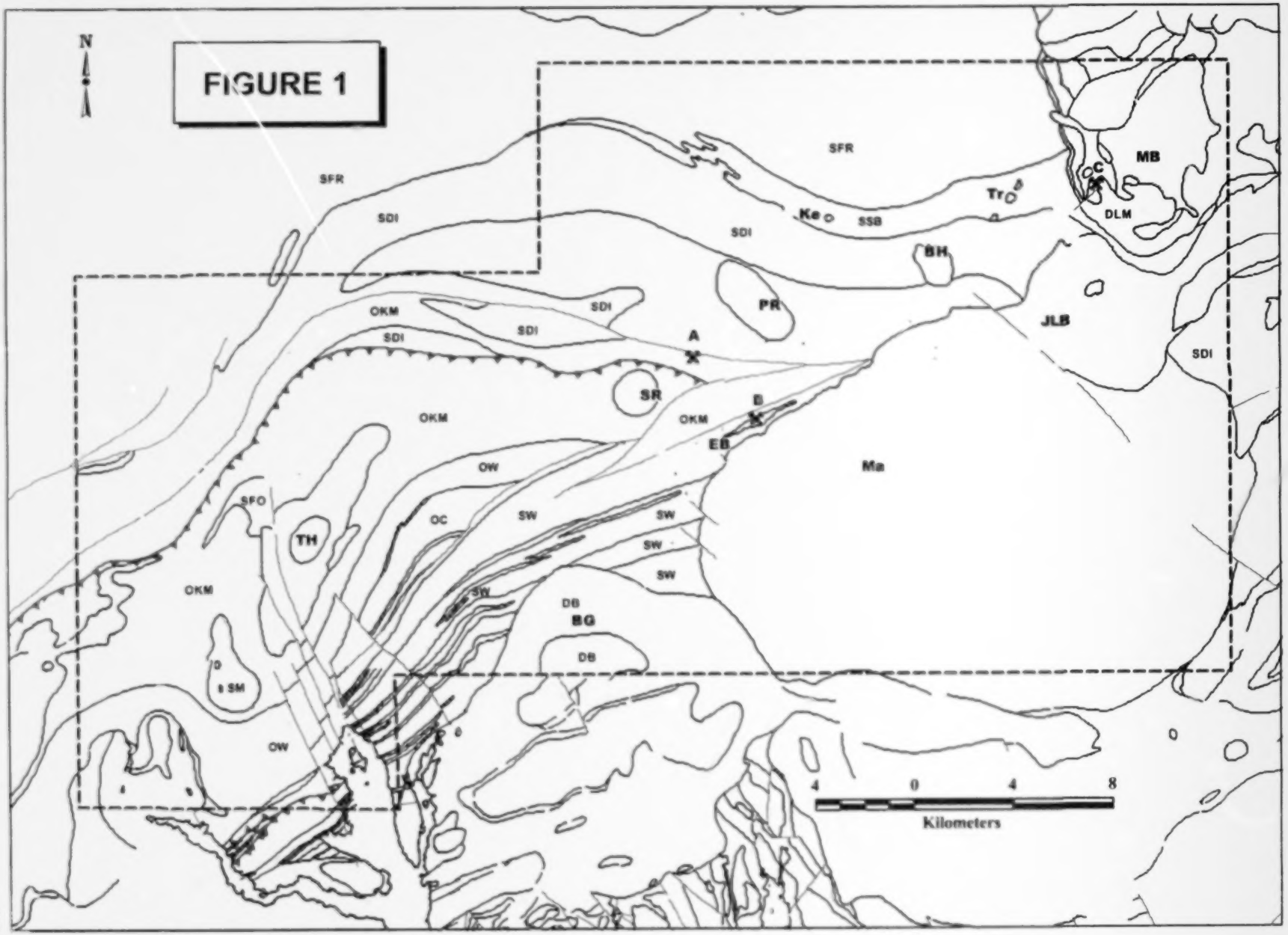
N
FIGURE 1
SFR
SDI
SFR
SDI
Ke
SSB
Tr
SDI
MB
CC
DLM
BH
PR
JLB
SDI
OKM
SDI
SDI
A
SR
B
OKM
OKM
EB
Ma
OW
SFO
TH
OC
SW
SW
SW
SW
OKM
SW
DB
BG
DB
SM
OW
4
0
4
8
Kilometers

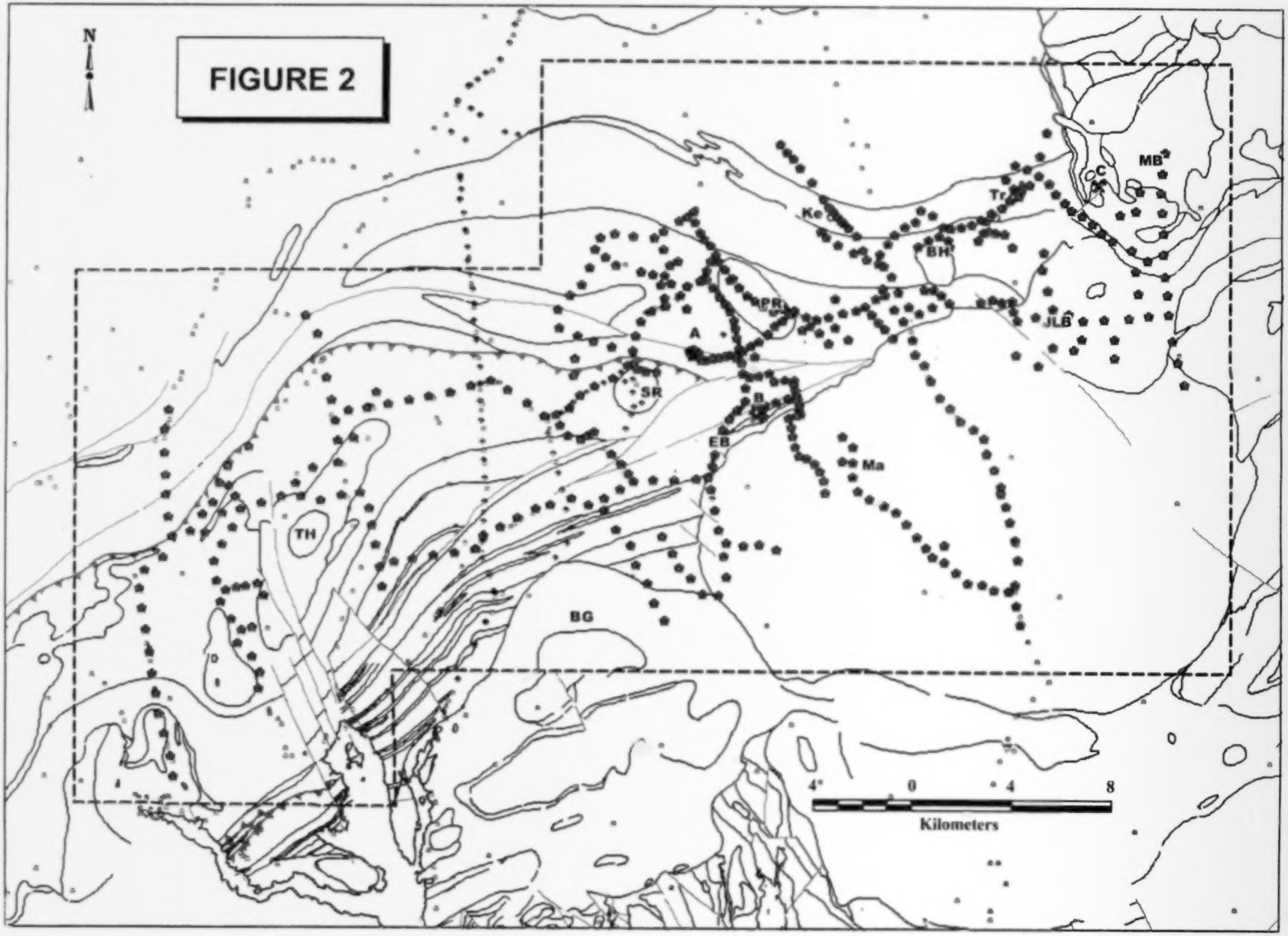
N
FIGURE 2
MB
C
Tr
Ke
BH
PR
A
JLB
SR
B
EB
Ma
TH
BG
4
0
4
8
Kilometers

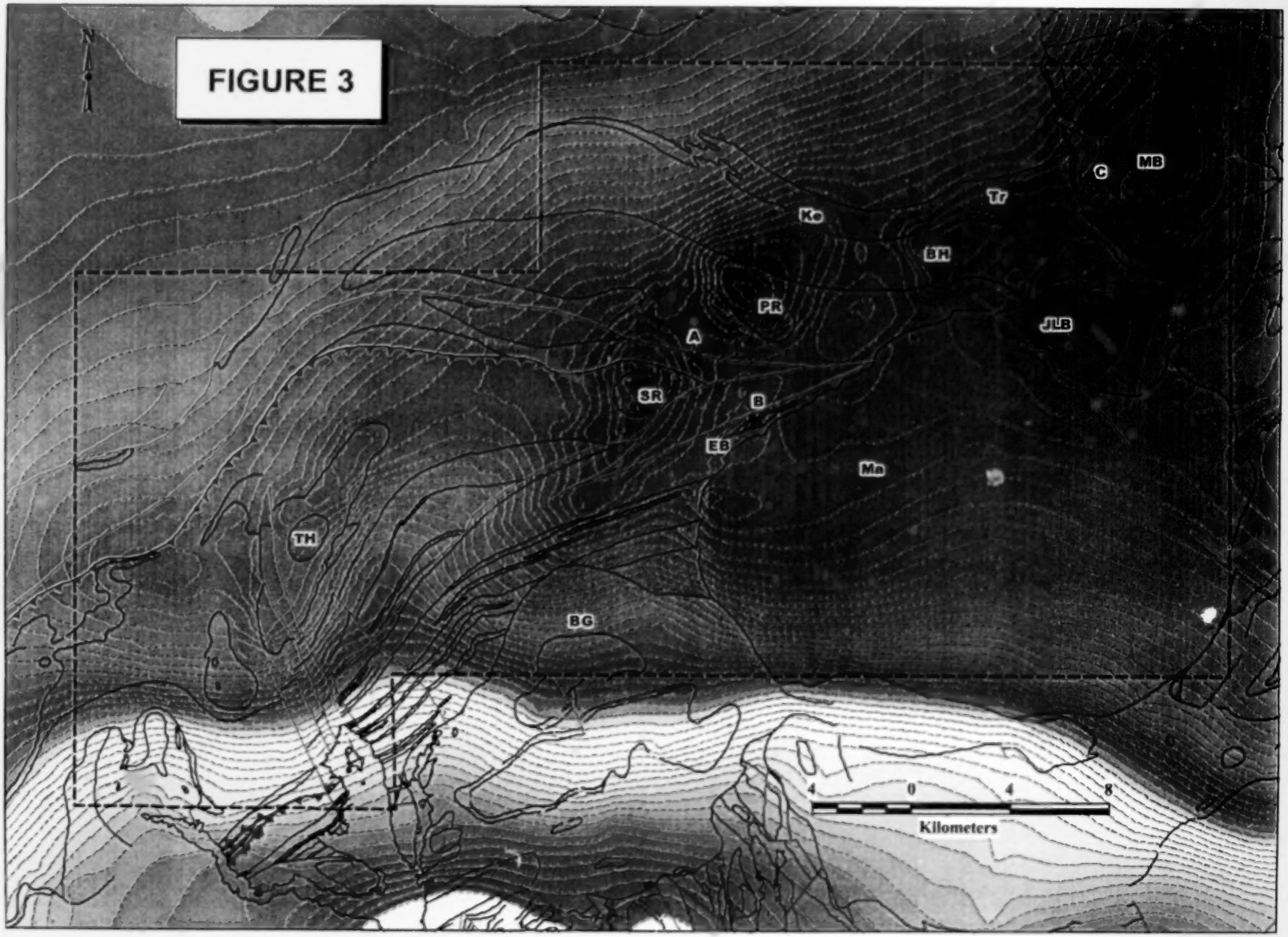
FIGURE 3
N
C
MB
Tr
Ko
BH
PR
JLB
A
SR
B
EB
Ma
TH
BG
4
0
4
8
Kilometers

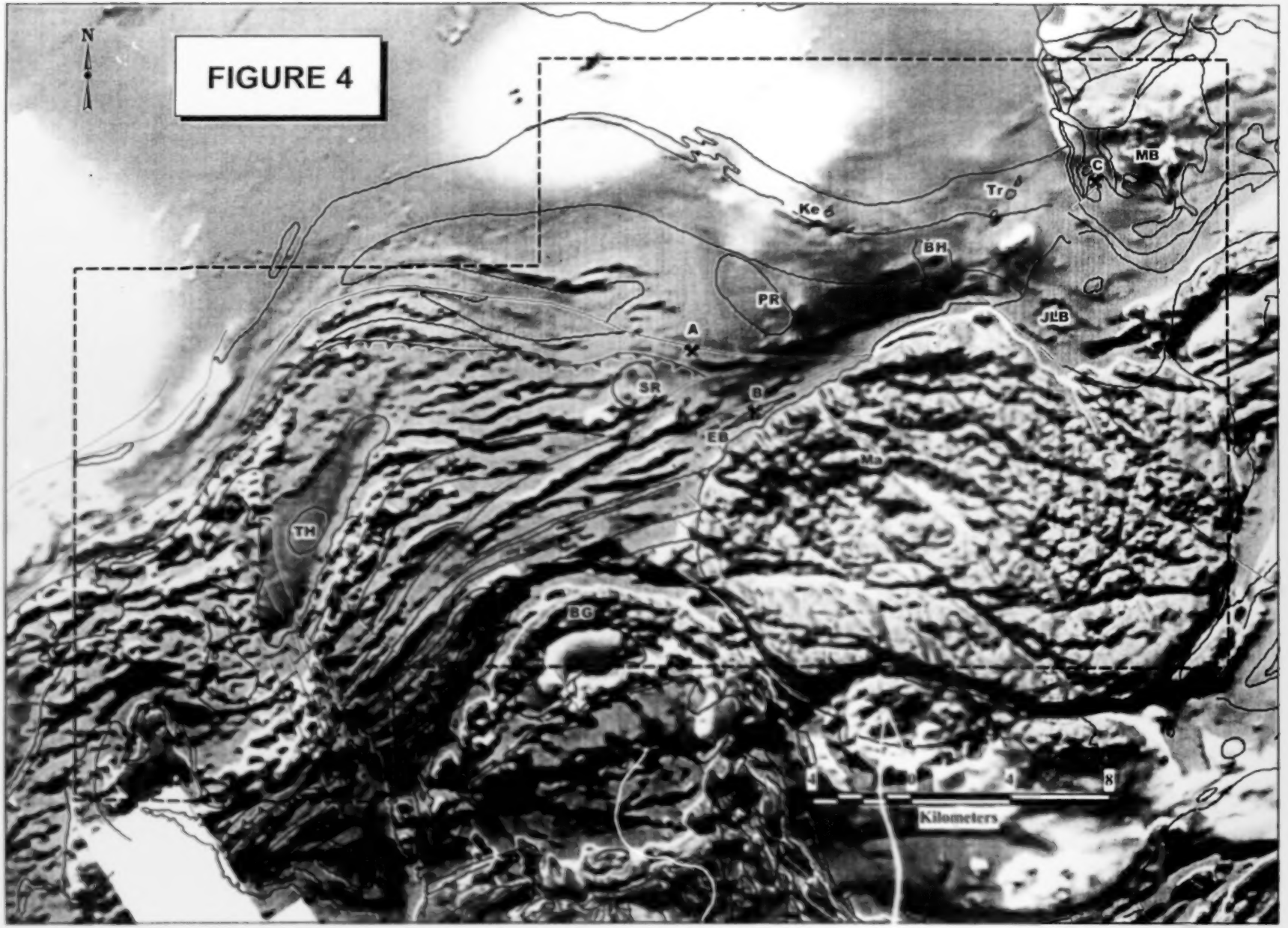
N
FIGURE 4
MB
C
Tr
Ke
BH
PR
JLB
A
SR
B
EB
Mb
TH
BG
4
4
8
Kilometers

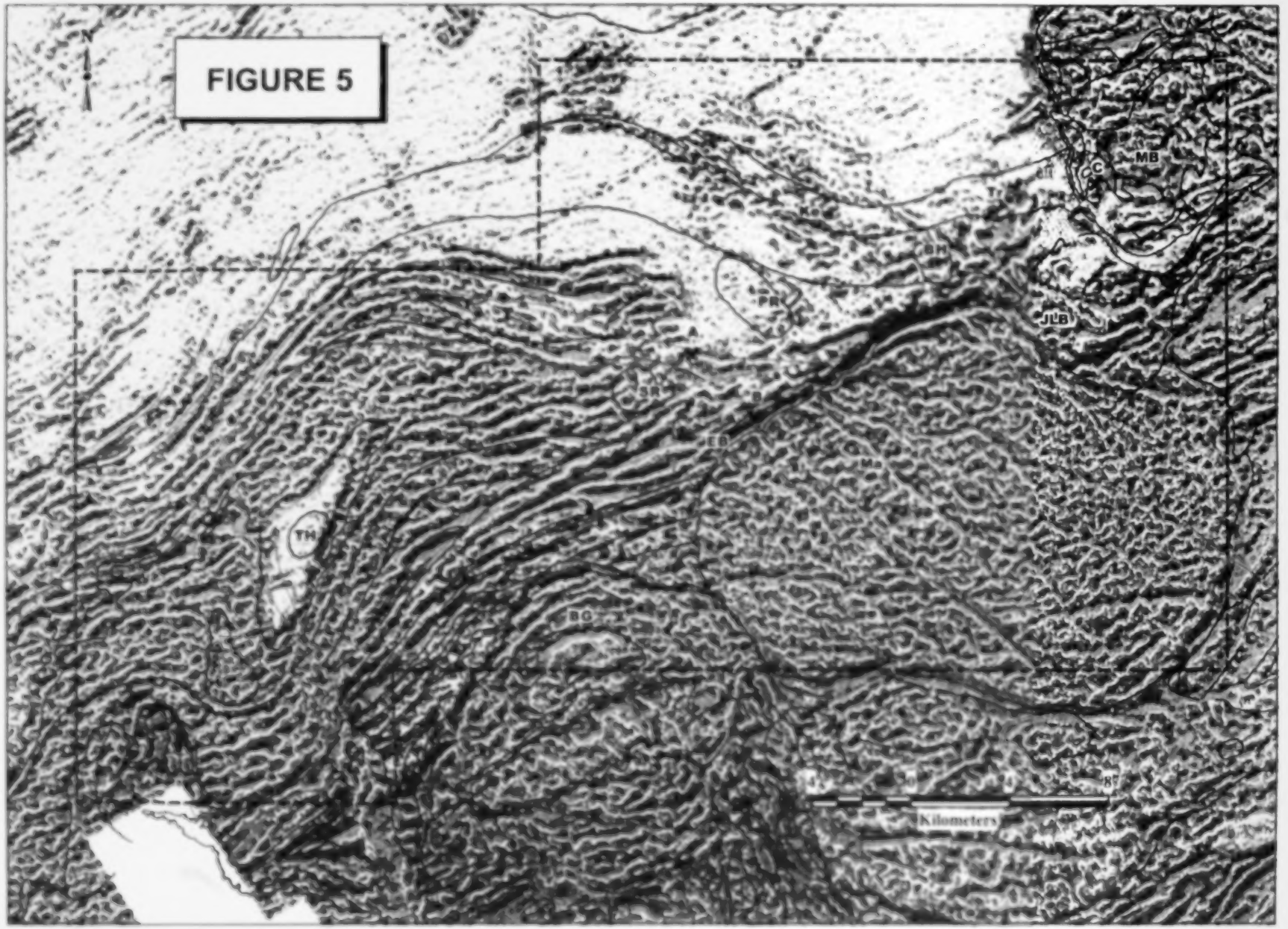
FIGURE 5
N
MB
C
BH
PR
JLB
SR
TH
BG
Kilometers

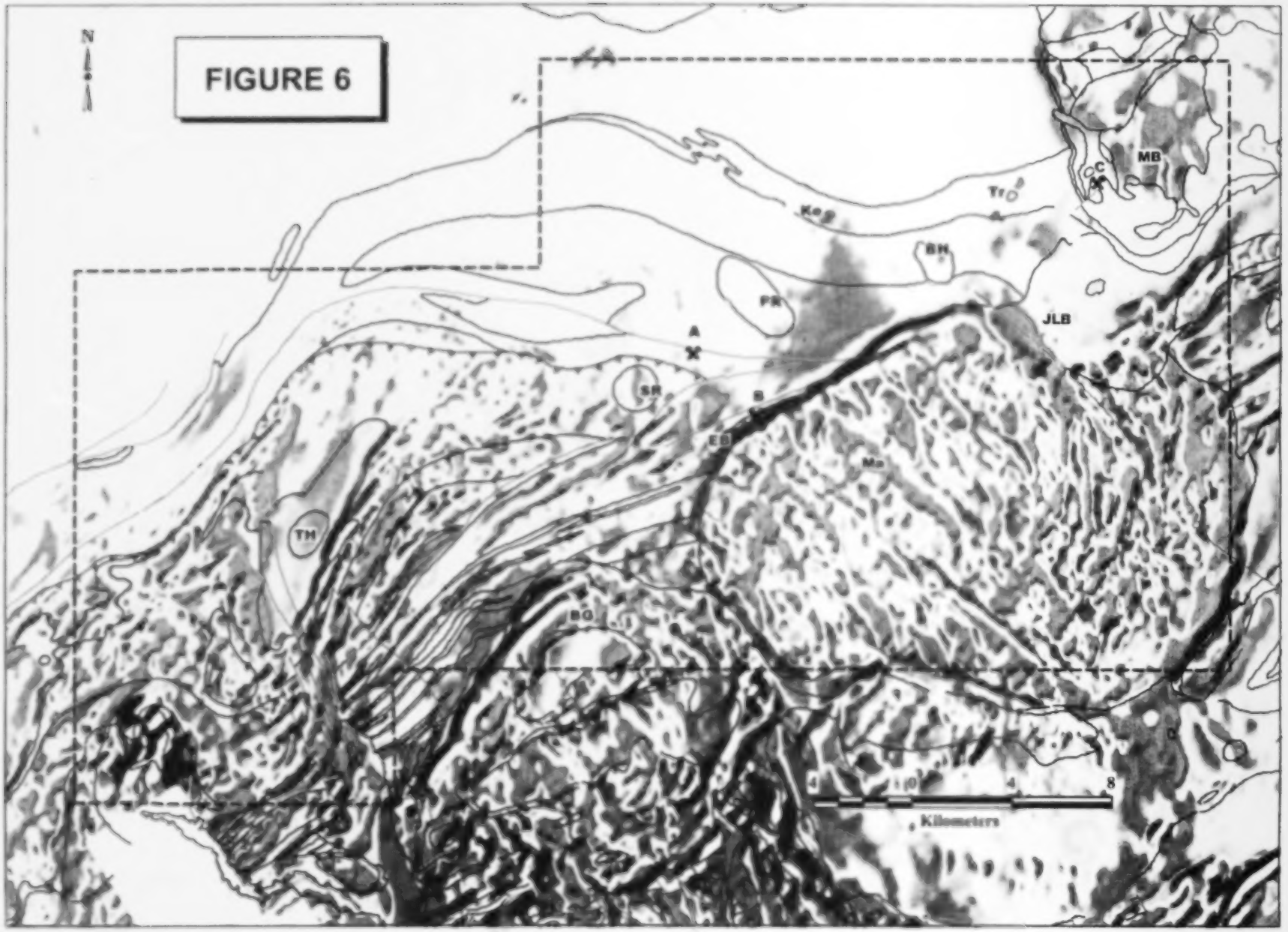
FIGURE 6
N
MB
C
Tr
Ko
BH
PR
JLB
SR
EB
Mo
TH
BO
0
4
8
Kilometers

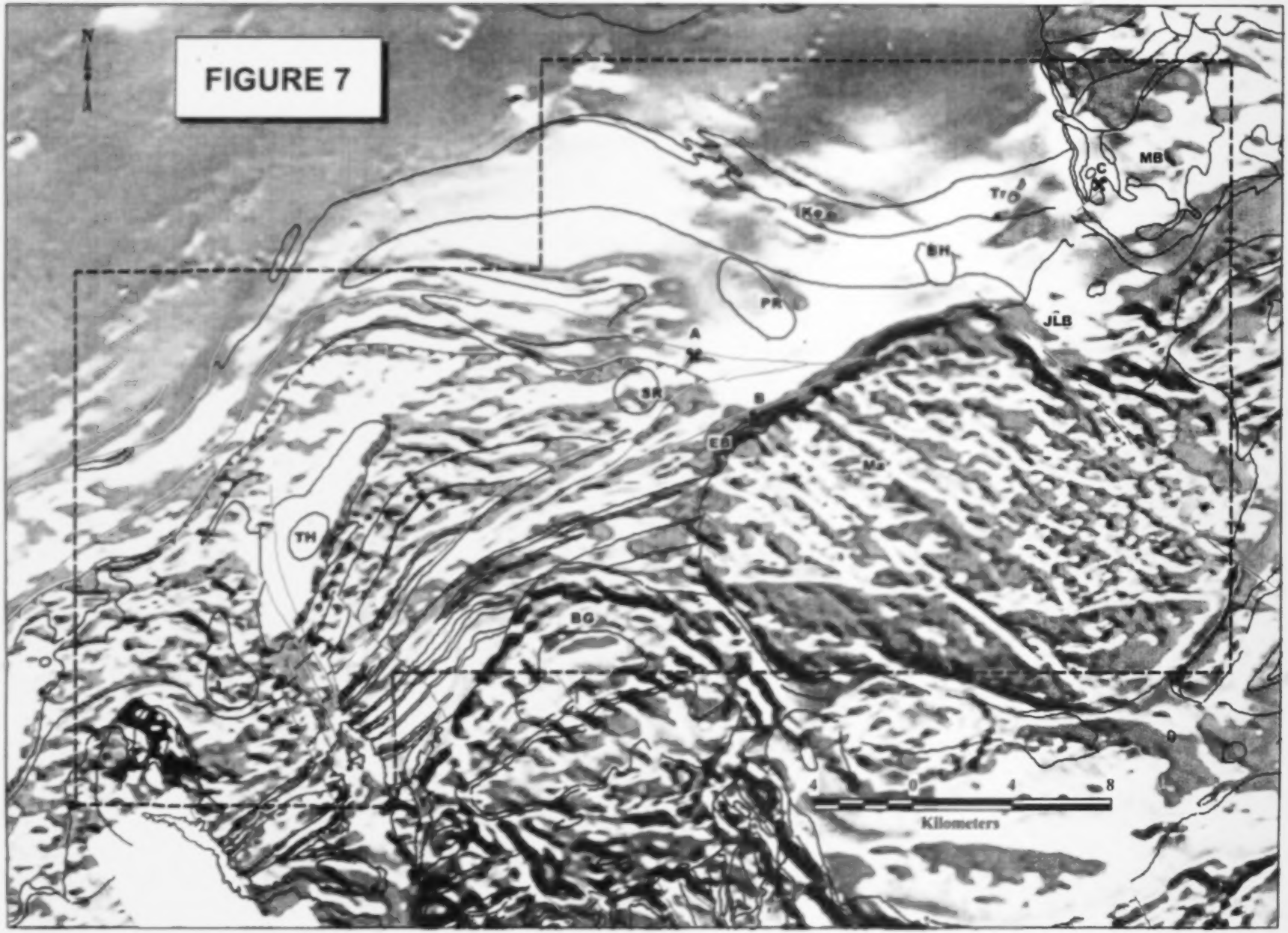
FIGURE 7
N
MB
CC
Tr
KQ
BH
PR
JLB
A
B
SR
EB
MP
TH
BG
4
0
4
8
Kilometers

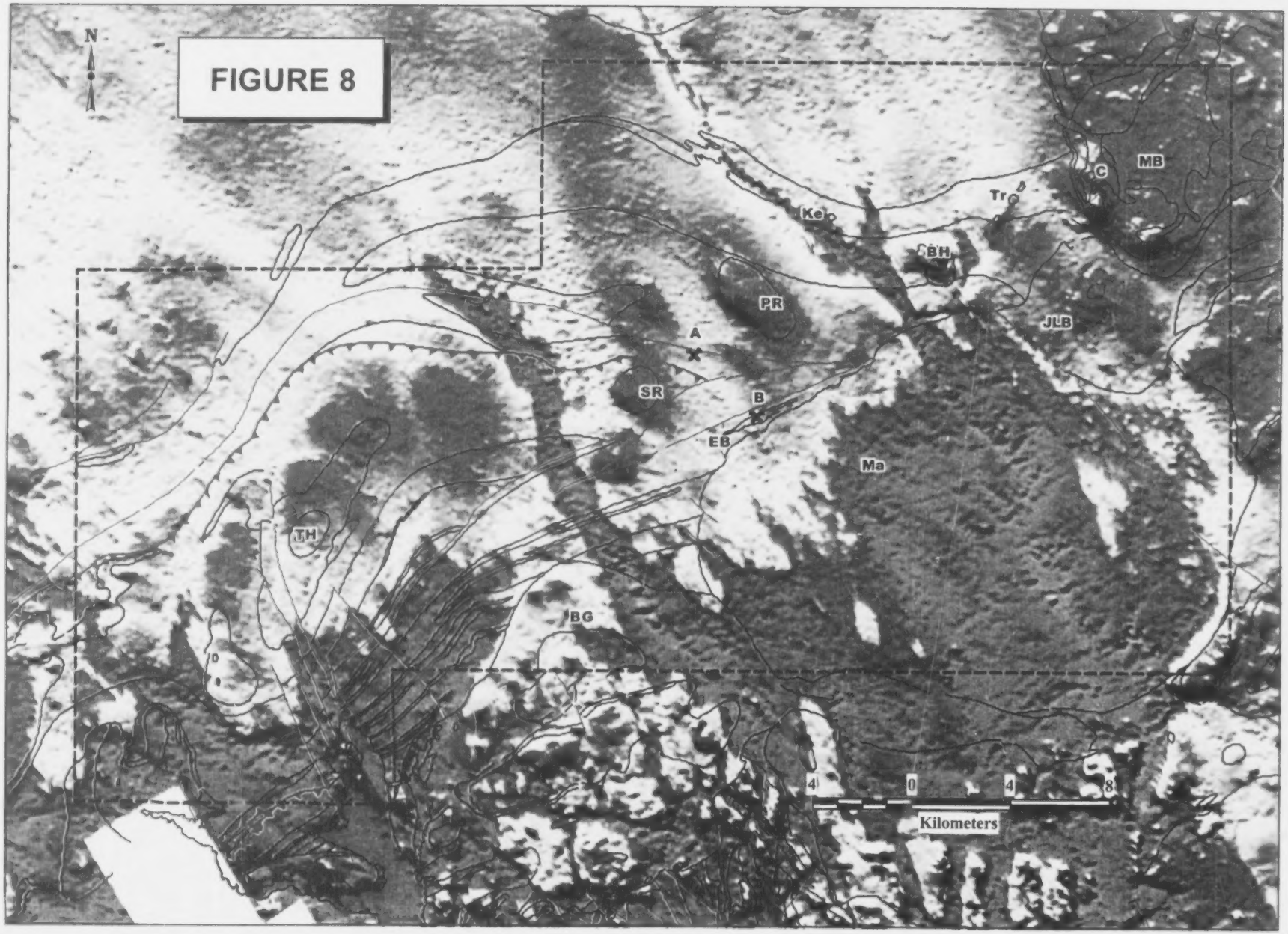
N
FIGURE 8
MB
C
Tr
Ke
CBH
PR
JLB
A
SR
B
EB
Ma
TH
BG
4
0
4
8
Kilometers

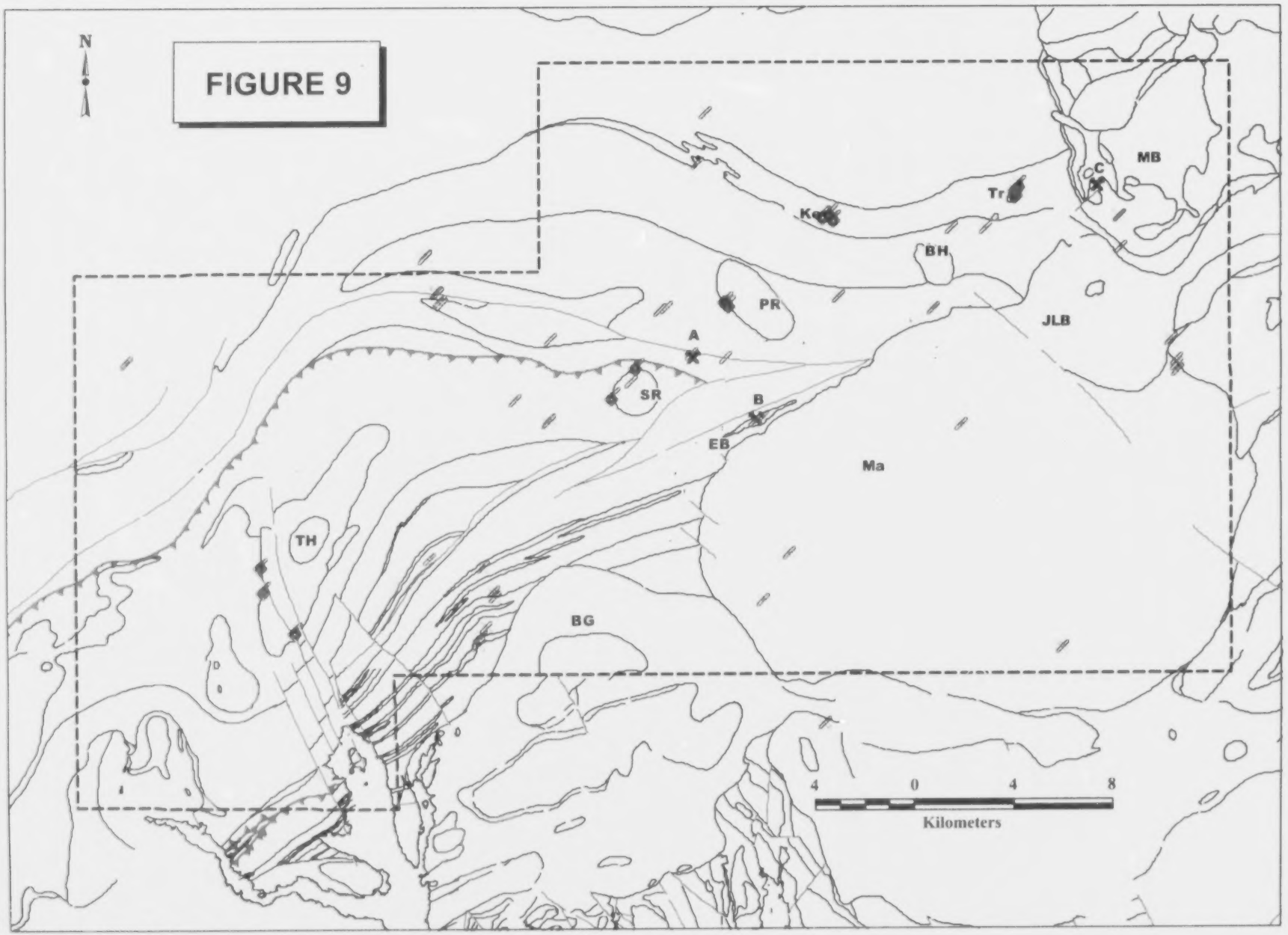
N
FIGURE 9
MB
C
Tr
K
BH
PR
JLB
A
SR
B
EB
Ma
TH
BG
4
0
4
8
Kilometers

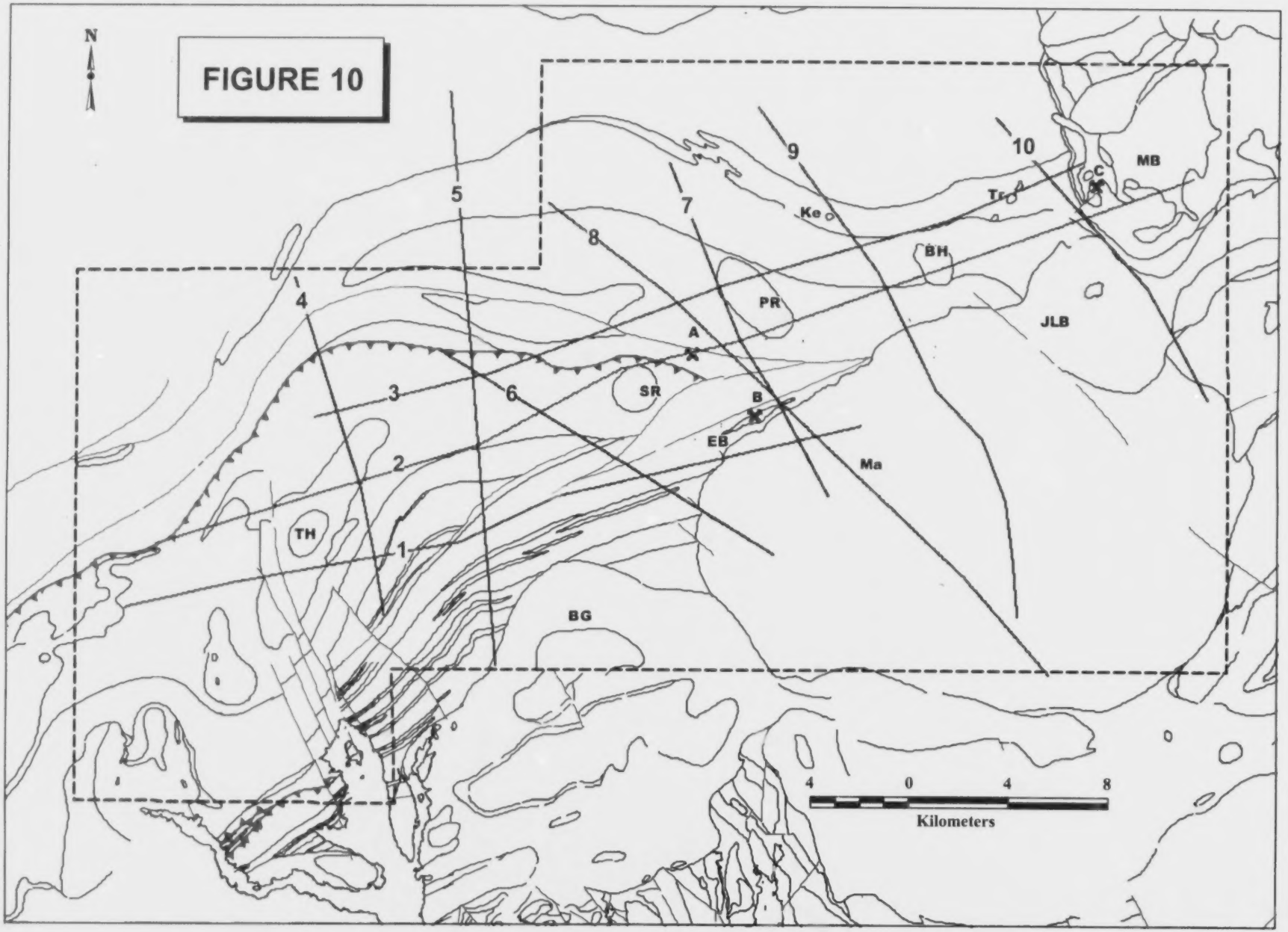
N
FIGURE 10
1
2
3
4
5
6
7
8
9
10
A
B
C
TH
SR
PR
BH
JLB
MB
Tr
Ke
EB
Ma
BG
4 0 4 8
Kilometers

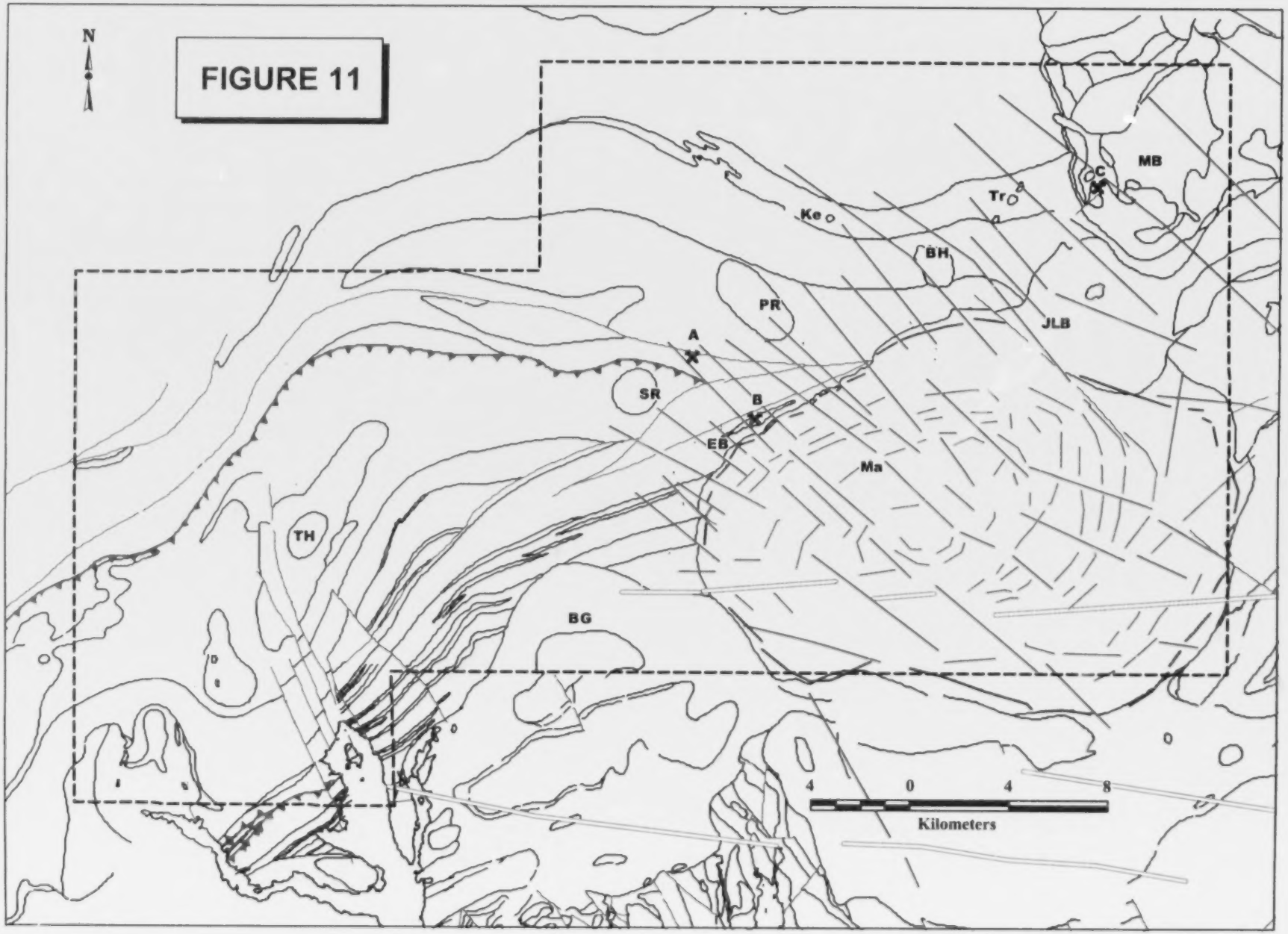
N
FIGURE 11
MB
C
Tr
Ke
BH
PR
JLB
A
SR
B
EB
Ma
TH
BG
4
0
4
8
Kilometers

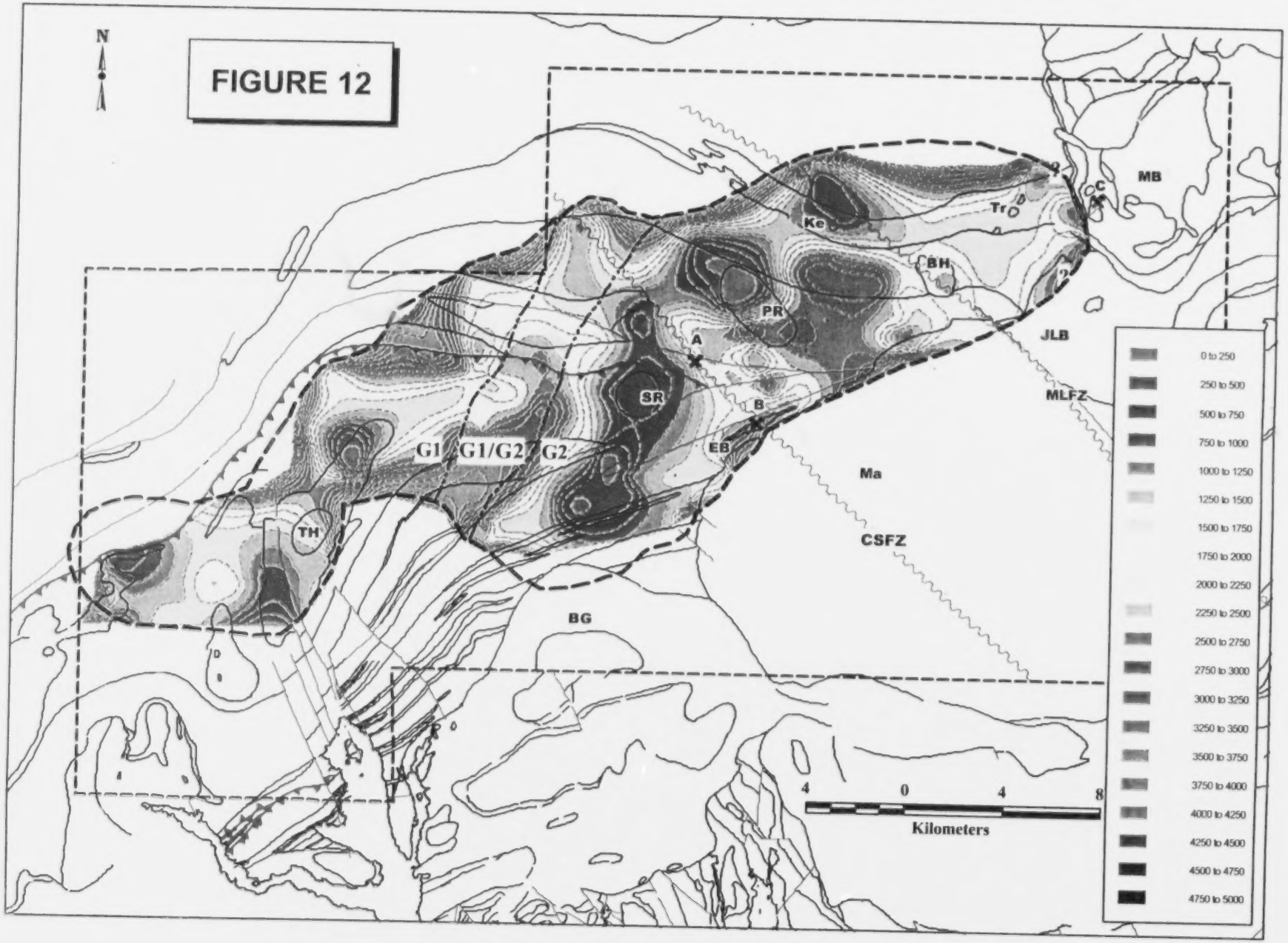
N
FIGURE 12
MB
Ke
Tr
BH
PR
JLB
A
SR
B
MLFZ
G1
G1/G2
G2
EB
Ma
CSFZ
TH
BG
4
0
4
8
Kilometers
0 to 250
250 to 500
500 to 750
750 to 1000
1000 to 1250
1250 to 1500
1500 to 1750
1750 to 2000
2000 to 2250
2250 to 2500
2500 to 2750
2750 to 3000
3000 to 3250
3250 to 3500
3500 to 3750
3750 to 4000
4000 to 4250
4250 to 4500
4500 to 4750
4750 to 5000

Appendix I: Gravity Survey Specifications and Digital Data

LOGISTICS REPORT

ACADIA UNIVERSITY
Regional Gravity Survey
St. Stephen, New Brunswick
Project Geophysicist: M. S. (Steve) King

Project # 0302

Ref: lr0302grv

Introduction

This field report covers the survey procedures and parameters for the regional gravity survey carried out for Acadia University in the St. Stephen area, in southwestern New Brunswick. This survey took place on various roads in an area previously scouted out by Steve King. The fact that Steve had previously mapped out the entire work area and then was part of the field crew, contributed greatly in the efficiency of this project. This logistics report deals with the fieldwork portion of this contract.

Survey Equipment

- 1 - LaCoste & Romberg model G gravity meter, Ser. # 789
- 1 - Leica\Wild SR399 Dual Frequency GPS Base Station
- 2 - Leica\Wild SR399E Dual Frequency GPS Rovers
- 1 - AcerNote Pentium laptop computer
    - Registered users of Geosoft^{tm} geophysical software
    - Registered users of Leica SKI^{tm} GPS software

Survey Specifications

- Regional Gravity Survey, along roads at intervals of 200, 400, 500, 600, and 800 meters.
- Gravity survey tied-in to a National Gravity Net station # 9158-73 located at the old Bank of Montreal building on the Corner of Water and Marks Streets, St. Stephen, NB.
- Gravity readings reduced to Bouguer mGal values
- Positioning from GPS Base Station tied in to local NBHPN monuments with differential GPS (Baseline lengths) located no further than 15 kilometers away.
- All coordinates are in the North American Datum 1983 (NAD 83) horizontal datum expressed in deg-mm-ssss format and UTM values in Zone 19.
- Elevations are in height above mean sea level (MSL)
- Maximum elevation tolerance of +/- 5 cm/ station
- Maximum gravity tolerance of 0.05 mGal/ station

Survey Procedure

A gravity observation and a precise DGPS X, Y, and Z position were obtained on strategically located roads in the survey area. Station intervals were set at a pre-determined amount based on geology. The station density varied throughout the survey. All the gravity data has been calculated or reduced to Bouguer mGal values. These calculations correct for the following parameters: (1) elevation, free-air correction, instrument height; (2) latitude correction; (3) tide correction on a daily basis; (4) instrument drift; and, if required (5) terrain corrections. For this contract, the gravity is tied-in to a National Gravity Network.

Gravity Base:

National Gravity Network base station:

- Station # 9158-73, value = 980622.29 mGal (Bank of Montreal St. Stephen, NB) Lat. 45° 11.59', Long. 67° 16.77', elev. = 7.00 m.

DGPS Control Points:

- Station Number: 941006 (Canadian Base Network)
  - Location: Moore's Mills - Lat. 45° 18' 29.2784", Long. 67° 14' 53.2404"
  - Orthometric height = 162.485 m.
- Station Number: 27946 (High Precision Densification station)
  - Location: Route 785 – Lat. 45° 22' 56.4511", Long. 66° 46' 15.9552"
  - Orthometric height = 108.365 m.
- Station Number: 1938 (High Precision Densification station)
  - Location: Pleasant 96 – Lat. 45° 23' 46.6641", Long. 66° 59' 59.1109"
  - Orthometric height = 279.868 m.

Note: The above values are in NAD83 (CSRS98) coordinates fixed to the Canadian Base Network (CBN) version 2.0 adjustment.

Personnel

Michael Tatlock and M.S. (Steve) King

EASTERN GEOPHYSICS LIMITED
GRAVITY REPEAT READINGS
ACADIA UNIVERSITY
REGIONAL GRAVITY SURVEY
ST. STEPHEN AREA, NB
PROJECT # 0302
METER # 789

Station	Loop	BS	Reading	Loop	BS	Reading	Diff.
2	6-10	99	-48.38	6-10	99	-48.39	.01
12	6-11	99	-47.18	6-10	99	-47.12	.06
2	6-11	99	-48.36	6-10	99	-48.38	.02
41	6-12	99	-38.31	6-11	99	-38.27	.04
100	6-14	99	-43.40	6-13	99	-43.40	.00
142	6-15	99	-44.67	6-14	99	-44.62	.05
24	6-16	99	-45.58	6-11	99	-45.54	.04
204	6-17	99	-41.85	6-16	99	-41.85	.00
258	6-18	99	-42.43	6-17	99	-42.43	.00
318	6-19	99	-41.57	6-18	99	-41.55	.02
358	6-20	99	-36.05	6-20	99	-36.04	.01
358	6-21	99	-36.06	6-20	99	-36.04	.02

EASTERN GEOPHYSICS LIMITED
GRAVITY LOOP CLOSURES
ACADIA UNIVERSITY
REGIONAL GRAVITY SURVEY
ST. STEPHEN AREA, NB
PROJECT # 0302
METER # 789

Loop	Base Start	Base End	Loop Time	Drift / Hour	Closure
6-10	99	99	6:30	-.0018	-.0119
6-11	99	99	9:28	.0005	.0049
6-12	99	99	10:33	-.0023	-.0246
6-13	99	99	12:22	-.0014	-.0173
6-14	99	99	13:04	-.0003	-.0042
6-15	99	99	11:56	-.0014	-.0171
6-16	99	99	10:39	.0027	.0283
6-17	99	99	10:34	.0040	.0425
6-18	99	99	13:03	-.0028	.0368
6-19	99	99	11:16	.0024	.0276
6-20	99	99	11:24	.0029	.0329
6-21	99	99	6:29	-.0082	-.0534

EASTERN GEOPHYSICS LIMITED
DGPS REPEAT READINGS
ACADIA UNIVERSITY
REGIONAL GRAVITY SURVEY
ST. STEPHEN AREA, NB
PROJECT # 0302
Leica SR 399 Dual Frequency DGPS System

Stn.	UTMX[1]	UTMY[1]	Elev.[1]	UTMX[2]	UTMY[2]	Elev.[2]	[3]Elev.+/-
12	656643.0295	5027645.360	154.1898	656643.0428	5027645.344	154.2430	+0.053
24	659185.2861	5027796.333	179.9282	659185.2853	5027796.303	179.9604	+0.032
41	653377.1712	5030348.166	138.1478	653377.1724	5030348.169	138.1366	-0.011
215	666796.3085	5023680.651	45.1519	666796.1744	5023680.868	45.1381	-0.014
258	659532.5334	5024687.284	133.4093	659532.5359	5024687.306	133.4176	+0.008
318	656978.5799	5023306.684	103.592	656978.5652	5023306.673	103.5966	+0.005
358	637360.3371	5018683.949	160.9683	637360.3246	5018683.936	160.9853	+0.017

[1]UTM Values in meters – Zone 19
[2]Elevations in meters – Height Above Mean Sea Level
[3]Quoted elevation tolerance for this survey = +/- 0.100 m.

Gravity Data

Gravity data are listed on subsequent nine pages.

Complete listing of new gravity data, southern New Brunswick (2003)

NAD83 UTMX	NAD83 UTMY	Station ID	Elevation (m)	Free Air Correction	Absolute Value	Bouguer Anomaly
656532.91	5028891.79	1	279.776	-17.15	980551.41	-48.45
656641.26	5028988.56	2	277.822	-17.29	980551.94	-48.38
656299.90	5029313.25	3	248.344	-19.82	980558.78	-47.61
656023.27	5029608.67	4	212.584	-22.84	980567.04	-46.63
655716.17	5029564.59	5	184.490	-25.05	980573.48	-45.69
655552.33	5029178.87	6	151.163	-27.84	980580.66	-44.75
655361.67	5028789.87	7	127.415	-29.60	980585.92	-43.85
655596.06	5028844.09	8	146.730	-28.42	980581.17	-44.84
655893.24	5028555.77	9	156.955	-28.49	980577.70	-46.06
656182.35	5028202.99	10	164.684	-28.75	980574.77	-47.18
656398.84	5027922.81	11	158.219	-29.71	980575.57	-47.41
656643.03	5027645.36	12	154.190	-29.87	980576.43	-47.12
656815.49	5027302.60	13	136.668	-31.11	980580.30	-46.41
656898.38	5026945.52	14	127.218	-31.18	980582.86	-45.42
656993.78	5026610.97	15	140.499	-28.85	980580.82	-44.57
657118.64	5026199.02	16	159.131	-26.04	980577.54	-43.84
657306.10	5026083.39	17	161.158	-25.68	980577.18	-43.71
657579.92	5026322.80	18	142.978	-28.19	980580.47	-44.19
657913.50	5026522.65	19	153.684	-27.53	980577.97	-44.73
658223.50	5026877.43	20	185.267	-25.12	980570.93	-45.85
658503.84	5027180.14	21	196.276	-24.41	980568.47	-46.38
658764.75	5027442.73	22	196.487	-24.33	980568.70	-46.31
659027.88	5027722.97	23	182.425	-25.57	980572.03	-45.98
659185.29	5027796.30	24	179.960	-25.44	980572.97	-45.58
659214.44	5027911.58	25	179.986	-25.54	980572.95	-45.68
658819.19	5027884.59	26	192.884	-24.88	980569.62	-46.47
658382.67	5027789.19	27	219.235	-22.83	980563.47	-47.36
657952.00	5027929.14	28	240.577	-21.39	980558.45	-48.31
657604.43	5028136.37	29	262.519	-19.25	980554.00	-48.62
657299.81	5028340.95	30	276.426	-17.87	980551.25	-48.80
656931.48	5028636.62	31	284.544	-16.83	980550.04	-48.67
655874.10	5029879.87	32	195.622	-24.08	980571.26	-45.97
655683.62	5030223.51	33	183.787	-23.72	980575.56	-44.28
655401.18	5030477.77	34	166.621	-23.99	980580.79	-42.64
655172.55	5030740.70	35	154.127	-23.64	980585.22	-40.89
654982.27	5031114.59	36	150.604	-22.57	980587.69	-39.42
654880.68	5031519.76	37	143.092	-21.98	980590.93	-37.99
654600.11	5031311.27	38	145.243	-21.67	980590.41	-37.92
654309.50	5031108.39	39	143.412	-21.65	980590.84	-37.70
653724.53	5030641.95	40	140.791	-22.29	980590.64	-38.04
653377.17	5030348.17	41	138.148	-22.81	980590.70	-38.27
653749.01	5029942.42	42	127.752	-25.21	980591.17	-39.50
654392.58	5029515.19	43	122.735	-27.34	980590.23	-41.07
652546.55	5030333.62	44	136.633	-22.61	980591.37	-37.90
651784.18	5030382.50	45	143.988	-21.58	980590.18	-37.70
651212.22	5030209.76	46	141.867	-22.08	980590.21	-37.96
651045.97	5029737.01	47	141.655	-22.82	980589.16	-38.67
651485.06	5029433.40	48	141.200	-23.44	980588.42	-39.24

651897.28	5029136.23	49	142.913	-23.80	980587.28	-39.79
650884.79	5028972.67	50	134.543	-24.86	980588.69	-39.91
650629.10	5028266.56	51	126.405	-26.76	980588.74	-40.90
650175.37	5027779.10	52	104.742	-29.42	980592.37	-41.14
649722.79	5027175.13	53	103.850	-29.33	980592.25	-40.95
649822.93	5026452.55	54	108.344	-29.91	980589.69	-42.04
650593.55	5026164.46	55	102.976	-30.86	980590.15	-42.38
651253.26	5026016.84	56	111.958	-30.69	980587.41	-43.22
651994.49	5025873.23	57	111.377	-32.63	980585.52	-45.09
650572.29	5025278.39	58	87.398	-33.05	980592.05	-42.83
650550.81	5024603.57	59	82.661	-33.97	980592.04	-43.22
654856.54	5028518.04	60	115.464	-30.09	980588.90	-43.01
654571.55	5028135.74	61	110.646	-31.04	980589.13	-43.42
654205.21	5028579.51	62	117.330	-29.44	980589.03	-42.57
653906.26	5028866.26	63	121.314	-28.27	980589.22	-41.84
653435.59	5028871.23	64	126.384	-27.59	980588.35	-41.73
652945.17	5028978.20	65	141.150	-25.09	980586.39	-40.88
653750.97	5028476.82	66	125.701	-28.83	980586.99	-42.90
653988.35	5027999.08	67	134.579	-28.61	980584.08	-43.67
654069.95	5029311.30	68	125.628	-27.04	980589.48	-41.09
654877.40	5027639.80	69	111.814	-31.26	980588.14	-43.77
674505.59	5027845.07	70	108.575	-29.64	980590.51	-41.79
674767.01	5027019.57	71	110.897	-29.08	980589.67	-41.49
675122.34	5026179.08	72	103.954	-31.97	980588.23	-43.61
674295.18	5028889.38	73	118.054	-29.52	980588.55	-42.73
673474.06	5028769.40	74	168.036	-24.41	980578.16	-43.22
672976.39	5029651.69	75	164.391	-25.07	980579.36	-43.47
672838.30	5030572.11	76	147.203	-26.21	980584.28	-42.68
672685.37	5028650.21	77	169.841	-25.13	980576.80	-44.14
672201.60	5027748.66	78	141.273	-28.91	980581.12	-44.72
672242.68	5027018.11	79	120.743	-30.96	980584.81	-44.47
671702.19	5028506.48	80	158.455	-26.83	980578.52	-44.56
670849.49	5028366.75	81	166.718	-26.13	980576.58	-44.79
670887.73	5027622.36	82	132.687	-29.88	980582.73	-44.73
670557.16	5027189.19	83	134.366	-30.07	980581.67	-45.11
669722.26	5027215.52	84	129.031	-30.91	980582.52	-45.35
669184.60	5026478.08	85	80.752	-34.57	980593.17	-43.61
668286.23	5026798.89	86	71.902	-35.58	980595.17	-43.63
670245.26	5028586.11	87	162.704	-26.93	980577.21	-45.13
669614.24	5028756.13	88	151.059	-27.86	980580.03	-44.76
669340.08	5029514.83	89	156.048	-26.63	980580.34	-44.09
669049.68	5030346.29	90	159.935	-25.86	980580.60	-43.75
669065.37	5031008.67	91	162.196	-24.83	980581.47	-42.98
668938.30	5028410.77	92	141.279	-29.28	980581.36	-45.09
668224.09	5028206.06	93	143.905	-29.00	980580.68	-45.11
668059.52	5028563.80	94	140.822	-29.11	980581.82	-44.87
667929.70	5028965.23	95	142.948	-28.38	980582.22	-44.38
667537.04	5028862.81	96	126.964	-29.32	980586.14	-43.53
667171.44	5028937.24	97	135.861	-28.28	980584.50	-43.48
666674.03	5028797.59	98	166.312	-25.23	980578.05	-43.84
674146.98	5029699.49	99	122.717	-29.80	980587.50	-43.53
674008.72	5030445.93	100	156.981	-25.84	980581.50	-43.40

673896.46	5031317.36	101	192.071	-21.17	980576.05	-42.66
673793.43	5032168.63	102	241.361	-16.55	980566.16	-43.55
673692.09	5032996.66	103	216.748	-19.80	980571.18	-44.05
673571.88	5033771.72	104	180.743	-24.58	980578.15	-44.80
673579.75	5034579.74	105	172.790	-25.84	980580.00	-45.17
673623.58	5035411.54	106	194.749	-23.23	980576.50	-45.02
672746.89	5033759.51	107	203.311	-22.98	980572.79	-45.73
672623.91	5032964.96	108	209.526	-21.78	980571.43	-45.23
672046.18	5032761.10	109	206.367	-22.24	980571.79	-45.33
673288.74	5031016.65	110	167.987	-23.98	980580.44	-42.78
672609.01	5031388.51	111	165.792	-24.68	980580.74	-43.24
671805.38	5031693.10	112	171.806	-24.00	980579.83	-43.23
671353.16	5031979.98	113	169.296	-25.69	980579.16	-44.63
670950.95	5032332.20	114	171.002	-25.51	980579.11	-44.64
670474.27	5032613.50	115	147.045	-28.16	980584.09	-44.62
670043.23	5032764.32	116	133.286	-29.69	980586.94	-44.60
669762.08	5033093.85	117	141.001	-28.69	980585.83	-44.46
669353.88	5033431.24	118	142.073	-28.81	980585.66	-44.71
669100.67	5033808.54	119	143.913	-28.25	980585.97	-44.35
668609.57	5034111.36	120	125.065	-29.37	980590.92	-43.37
668623.97	5034889.86	121	142.179	-25.55	980590.09	-41.46
668813.77	5035886.02	122	147.994	-24.00	980590.65	-40.56
668120.38	5034318.35	123	113.404	-29.07	980595.00	-41.76
667670.84	5034469.65	124	113.080	-28.59	980595.71	-41.24
668263.20	5033701.85	125	112.963	-31.40	980592.30	-44.04
663991.58	5030852.06	126	155.497	-28.77	980579.57	-46.17
664392.32	5031113.85	127	120.285	-32.11	980587.31	-45.57
664784.59	5031346.26	128	110.235	-33.01	980589.69	-45.35
665255.73	5030948.26	129	116.003	-34.40	980586.19	-47.38
665210.12	5031201.56	130	103.569	-34.93	980589.70	-46.52
665260.09	5031684.81	131	86.172	-35.91	980594.48	-45.55
665672.86	5031776.12	132	85.514	-36.63	980594.03	-46.19
666097.52	5031918.02	133	108.757	-33.47	980590.12	-45.64
666452.53	5032117.42	134	132.915	-30.38	980585.91	-45.26
666653.14	5032129.41	135	154.111	-27.79	980581.97	-45.03
666572.78	5031646.49	136	129.708	-31.09	980585.81	-45.60
666424.98	5031275.60	137	95.224	-34.82	980592.42	-45.48
666777.23	5031711.78	138	162.316	-27.35	980579.53	-45.51
667060.63	5031642.04	139	171.135	-25.63	980578.47	-44.78
667438.52	5031653.35	140	173.303	-25.08	980578.36	-44.47
667777.56	5031112.81	141	158.782	-25.51	980581.96	-43.27
666859.96	5032433.97	142	153.830	-27.41	980582.68	-44.62
667255.12	5032658.33	143	152.130	-27.66	980583.13	-44.68
667525.73	5032994.83	144	144.272	-28.51	980584.97	-44.65
667876.93	5033209.04	145	130.753	-30.13	980587.69	-44.76
667990.95	5033493.98	146	114.830	-31.48	980591.48	-44.33
667674.35	5033531.64	147	114.878	-31.42	980591.57	-44.27
667334.68	5033831.50	148	115.004	-29.28	980593.92	-42.15
661537.46	5022947.29	149	75.071	-34.69	980592.09	-43.09
662015.89	5022569.00	150	64.706	-35.74	980593.93	-42.98
662045.64	5021956.92	151	68.418	-35.18	980592.83	-42.84
661627.20	5021984.21	152	78.566	-34.16	980590.75	-42.95

662129.41	5021343.20	153	70.448	-34.88	980592.01	-42.76
662360.35	5020789.79	154	64.038	-35.42	980592.99	-42.58
662845.63	5020532.50	155	66.703	-34.76	980592.61	-42.23
663472.54	5020301.06	156	58.406	-35.21	980594.52	-41.75
663967.85	5020090.33	157	55.363	-35.17	980595.32	-41.36
664404.36	5019638.05	158	55.129	-34.49	980595.69	-40.66
664863.52	5019155.58	159	53.998	-33.90	980596.23	-39.94
665264.06	5018735.26	160	54.600	-33.02	980596.57	-39.13
665581.34	5018407.66	161	54.448	-32.26	980597.11	-38.35
666020.10	5018907.60	162	67.253	-31.37	980594.45	-38.89
666059.77	5018214.34	163	61.480	-30.80	980596.23	-37.67
666538.58	5017813.29	164	58.450	-30.11	980597.51	-36.65
667070.27	5017439.78	165	61.086	-29.01	980597.49	-35.84
667661.37	5017411.24	166	49.600	-29.95	980600.06	-35.50
668128.26	5017277.97	167	51.098	-29.53	980599.89	-35.25
668718.73	5017249.83	168	54.672	-29.26	980599.02	-35.38
669103.43	5016715.33	169	53.295	-28.68	980599.59	-34.65
669307.69	5015947.55	170	54.542	-27.29	980599.96	-33.40
668993.98	5017518.81	171	52.100	-29.89	980599.40	-35.72
668980.10	5018527.11	172	49.125	-31.65	980599.38	-37.15
668833.13	5019332.77	173	40.445	-33.73	980600.64	-38.26
668539.19	5020069.26	174	35.650	-35.11	980601.35	-39.10
668384.19	5020648.20	175	50.267	-34.23	980598.18	-39.86
668134.55	5021178.76	176	53.535	-34.17	980597.68	-40.16
659725.60	5027641.64	177	152.716	-26.48	980580.20	-43.57
660133.54	5027611.08	178	136.327	-27.26	980584.45	-42.51
659598.93	5027108.50	179	154.857	-26.23	980579.36	-43.56
659907.87	5027317.24	180	148.409	-26.23	980581.51	-42.84
660302.55	5027047.57	181	141.304	-25.92	980583.79	-41.73
660679.93	5026668.81	182	139.207	-25.66	980584.38	-41.24
660603.68	5027734.10	183	118.808	-28.25	980588.95	-41.55
660928.01	5027335.11	184	132.576	-26.13	980586.49	-40.97
661464.15	5026897.09	185	141.635	-24.98	980584.47	-40.83
660812.40	5028498.84	186	109.760	-29.23	980591.38	-41.51
661202.22	5027930.94	187	128.922	-26.36	980587.86	-40.79
661688.41	5028088.15	188	136.450	-25.00	980587.02	-40.27
662088.08	5028275.08	189	134.946	-24.93	980587.70	-40.03
662364.84	5027982.62	190	147.563	-23.73	980584.77	-40.24
662662.76	5027671.70	191	152.437	-23.56	980583.17	-40.61
662919.50	5027405.51	192	143.659	-24.80	980584.42	-40.87
663255.05	5027050.17	193	126.112	-28.56	980585.78	-42.67
662466.93	5028616.18	194	107.400	-28.32	980593.08	-40.34
662717.10	5029035.00	195	55.579	-34.63	980603.10	-40.85
663334.74	5028920.37	196	66.570	-34.28	980599.96	-41.72
663786.01	5028412.02	197	63.468	-34.67	980600.09	-41.77
664260.97	5028154.10	198	67.021	-34.82	980598.62	-42.32
664731.73	5028450.75	199	112.156	-30.30	980589.46	-42.85
665403.45	5028679.74	200	97.148	-32.88	980591.68	-43.75
665103.31	5028977.75	201	101.310	-32.44	980591.08	-43.77
664781.49	5029172.15	202	104.565	-32.62	980590.06	-44.32
664401.31	5029142.38	203	109.269	-31.35	980589.87	-43.57
663024.98	5029533.99	204	67.676	-34.28	980600.11	-41.85

662828.79	5028770.15	205	60.306	-33.95	980602.10	-40.70
663222.08	5028249.04	206	74.960	-32.59	980598.51	-40.97
663637.68	5027785.01	207	67.043	-34.26	980598.89	-41.77
664065.80	5027085.36	208	70.235	-35.64	980595.95	-43.50
664224.49	5026524.38	209	81.308	-34.21	980593.50	-43.31
664598.18	5026096.98	210	72.839	-35.25	980594.72	-43.40
664935.29	5025506.28	211	66.144	-36.11	980595.44	-43.51
665349.17	5024867.47	212	61.349	-36.29	980596.21	-43.15
665820.55	5024467.49	213	59.076	-36.24	980596.62	-42.85
666265.68	5023983.30	214	57.105	-36.21	980596.86	-42.60
666796.31	5023680.65	215	45.152	-37.20	980599.30	-42.25
667245.25	5023317.08	216	47.623	-36.55	980598.89	-41.87
667405.03	5022729.04	217	63.629	-34.44	980595.57	-41.56
662664.05	5029951.27	218	69.627	-33.72	980600.42	-41.51
662468.84	5030401.42	219	70.939	-33.52	980600.59	-41.46
662759.37	5030852.43	220	81.643	-33.08	980598.08	-42.22
663017.14	5031273.98	221	85.950	-32.91	980597.26	-42.53
663423.81	5031608.65	222	99.218	-31.57	980594.77	-42.68
663824.29	5031830.76	223	106.257	-30.92	980593.42	-42.81
664013.11	5032326.99	224	106.475	-29.83	980594.84	-41.75
664475.23	5032130.64	225	115.863	-29.69	980591.92	-42.65
664949.34	5031706.05	226	109.601	-32.74	980590.44	-45.01
662486.08	5030054.82	227	69.531	-33.77	980600.49	-41.55
661971.46	5030173.82	228	57.957	-34.64	980603.30	-41.12
661768.13	5030544.03	229	71.550	-32.97	980601.08	-40.97
661479.59	5031063.88	230	87.603	-31.54	980597.99	-41.34
661149.22	5031351.96	231	88.621	-31.77	980597.68	-41.69
660921.40	5031549.48	232	91 596	-31.80	980596.90	-42.05
660776.68	5031677.70	233	92.570	-31.82	980596.69	-42.18
660637.84	5031798.86	234	92.065	-31.95	980596.82	-42.25
660451.58	5032003.36	235	91.151	-31.88	980597.34	-42.08
660307.80	5032167.43	236	90.549	-31.81	980597.73	-41.94
660048.53	5032470.31	237	91.552	-31.25	980598.23	-41.49
659506.06	5033098.65	238	93.322	-29.96	980599.50	-40.40
659014.37	5033671.31	239	99.590	-27.51	980600.49	-38.65
658412.95	5034268.85	240	102.814	-24.48	980603.02	-35.99
658125.05	5034555.17	241	106.402	-23.09	980603.55	-34.99
658698.22	5033991.16	242	102.147	-25.80	980601.68	-37.23
661446.95	5030367.19	243	65.141	-34.53	980601.36	-41.82
660798.02	5030667.61	244	70.109	-35.54	980599.08	-43.38
660274.01	5030939.04	245	68.323	-37.04	980598.36	-44.69
660036.13	5031123.64	246	72.837	-37.02	980597.14	-45.17
667800.84	5022112.73	247	69.955	-33.16	980594.39	-40.99
668086.15	5021433.74	248	62.200	-33.48	980595.90	-40.44
657263.31	5025626.72	249	158.419	-25.17	980578.16	-42.90
657371.89	5025213.13	250	133.847	-27.20	980583.37	-42.18
657636.98	5025059.45	251	136.765	-26.62	980582.92	-41.93
658003.21	5025159.09	252	149.566	-25.19	980580.48	-41.93
658422.67	5025273.22	253	146.476	-25.63	980581.08	-42.02
658653.92	5024999.16	254	141.720	-25.79	980582.15	-41.65
659070.75	5025072.14	255	138.311	-26.39	980582.66	-41.87
659417.98	5025090.75	256	138.304	-26.55	980582.50	-42.03

659476.58	5024880.72	257	137.706	-26.79	980582.28	-42.20
659532.53	5024687.28	258	133.409	-27.51	980582.73	-42.43
659592.49	5024492.63	259	125.065	-28.67	980583.99	-42.66
659644.05	5024301.03	260	124.395	-29.18	980583.52	-43.10
659711.19	5024065.05	261	123.485	-29.80	980582.99	-43.62
659767.44	5023863.51	262	119.586	-30.31	980583.52	-43.69
659784.05	5023714.95	263	118.376	-30.58	980583.50	-43.82
659645.65	5023664.04	264	112.347	-31.32	980584.58	-43.89
659352.69	5023532.82	265	125.219	-29.98	980581.85	-43.99
659449.33	5023203.78	266	115.928	-30.86	980583.57	-43.83
659565.17	5022821.65	267	103.537	-31.99	980585.94	-43.58
659678.25	5022429.66	268	99.812	-32.30	980586.46	-43.47
659898.08	5022070.39	269	86.582	-33.64	980588.91	-43.33
660189.30	5021956.21	270	86.285	-33.56	980588.98	-43.22
660539.92	5021803.05	271	77.798	-34.39	980590.64	-43.09
660764.65	5021463.27	272	78.635	-34.27	980590.22	-43.07
660966.97	5021115.61	273	80.877	-33.89	980589.62	-42.94
661034.01	5020631.24	274	88.733	-33.09	980587.60	-43.02
659210.87	5024307.80	275	129.676	-27.80	980583.29	-42.31
658750.69	5024165.89	276	142.469	-25.97	980581.07	-41.91
658326.87	5024024.67	277	143.709	-25.75	980580.79	-41.83
657996.74	5023936.00	278	127.116	-27.40	980584.20	-41.63
658283.42	5023782.54	279	130.851	-26.81	980583.51	-41.45
658350.23	5023514.37	280	126.184	-27.91	980583.63	-42.03
657802.87	5025949.44	281	151.789	-26.49	980579.14	-43.47
657029.64	5025799.27	282	155.549	-25.70	980578.66	-43.11
656755.76	5025877.15	283	145.708	-26.92	980580.55	-43.23
656561.48	5025845.64	284	135.397	-28.01	980582.62	-43.16
656330.77	5025777.32	285	122.926	-29.45	980584.97	-43.21
656053.38	5025697.38	286	109.376	-31.12	980587.42	-43.36
655801.88	5025639.94	287	106.546	-31.75	980587.63	-43.67
655624.49	5025624.33	288	107.112	-31.88	980587.31	-43.87
655514.95	5025750.77	289	107.542	-32.08	980587.08	-44.12
655490.38	5025936.79	290	114.000	-31.50	980585.82	-44.26
655361.71	5026002.76	291	112.442	-31.63	980586.23	-44.21
655270.26	5025991.41	292	114.619	-31.59	980585.59	-44.42
655142.48	5025924.91	293	118.337	-31.46	980584.53	-44.70
655240.12	5025752.29	294	113.125	-32.03	980585.42	-44.69
654035.50	5027669.02	295	158.144	-26.16	980578.98	-43.86
653465.38	5027420.18	296	184.035	-23.78	980573.18	-44.38
653112.14	5026958.62	297	149.161	-28.45	980578.91	-45.14
652928.87	5026377.87	298	170.265	-27.00	980573.38	-46.05
652879.30	5025754.52	299	159.822	-30.25	980572.84	-48.13
652919.28	5025257.05	300	174.774	-29.32	980568.75	-48.88
653074.21	5025016.91	301	185.001	-28.48	980566.24	-49.18
653466.76	5024977.11	302	176.359	-29.31	980568.03	-49.04
653888.04	5024972.02	303	164.435	-30.22	980570.79	-48.62
652700.45	5025183.96	304	165.802	-30.14	980570.64	-48.70
652145.85	5024579.57	305	140.835	-31.14	980576.87	-46.90
651437.35	5024223.57	306	94.611	-34.34	980587.65	-44.93
650899.77	5023808.87	307	79.877	-34.82	980591.40	-43.75
650508.82	5023281.11	308	80.054	-33.77	980591.97	-42.73

649972.60	5022965.59	309	70.126	-34.32	980594.24	-42.17
650172.70	5022536.87	310	70.046	-35.08	980593.15	-42.92
650546.69	5022123.72	311	96.993	-33.13	980586.44	-43.98
651066.54	5022027.39	312	104.823	-33.22	980583.84	-44.95
651321.17	5022229.24	313	117.115	-32.38	980581.05	-45.48
651585.17	5022395.66	314	120.134	-32.57	980580.06	-46.01
657513.05	5024652.22	315	124.003	-27.69	980585.46	-41.57
657563.70	5024102.99	316	112.337	-28.64	980587.66	-41.21
657266.18	5023724.37	317	107.626	-29.34	980588.12	-41.38
656978.58	5023306.68	318	103.592	-29.96	980588.41	-41.55
656762.19	5022856.48	319	101.254	-30.75	980587.98	-42.08
656541.88	5022382.93	320	98.247	-31.42	980587.85	-42.42
656475.83	5021844.52	321	94.702	-32.16	980587.77	-42.76
656427.65	5021370.71	322	99.359	-31.89	980586.22	-43.00
656308.67	5020902.67	323	123.462	-28.85	980581.44	-42.67
656446.44	5020404.35	324	114.328	-30.08	980582.62	-42.87
656662.52	5019581.66	325	103.727	-31.25	980584.05	-42.86
656864.05	5018800.02	326	114.236	-29.54	980581.87	-42.33
657253.85	5018280.62	327	92.638	-31.12	980586.53	-41.48
657934.35	5018242.92	328	93.019	-31.05	980586.44	-41.46
658562.32	5018334.93	329	93.279	-31.18	980586.29	-41.62
659283.79	5018199.90	330	90.243	-31.29	980586.99	-41.39
657149.14	5017759.45	331	66.661	-33.22	980592.02	-40.68
657337.11	5016937.43	332	67.144	-31.41	980593.01	-38.92
657067.12	5016152.34	333	94.968	-25.30	980589.90	-35.93
656469.38	5016159.77	334	103.172	-22.57	980590.12	-34.11
655911.82	5016748.00	335	111.093	-24.07	980586.67	-36.50
655435.34	5017163.42	336	84.171	-28.01	980591.38	-37.43
655089.42	5017734.20	337	81.197	-29.28	980591.50	-38.37
654642.83	5018389.27	338	80.732	-30.34	980591.12	-39.37
655003.74	5015009.55	339	43.695	-24.21	980605.92	-29.10
654529.90	5015681.96	340	45.356	-25.46	980604.72	-30.54
654178.56	5016420.11	341	50.476	-28.69	980600.52	-34.34
653683.37	5017151.31	342	54.609	-30.92	980597.61	-37.03
653380.52	5017905.89	343	63.753	-32.21	980594.13	-39.34
652764.23	5018497.87	344	69.855	-34.26	980590.69	-42.07
652259.44	5019228.75	345	86.421	-34.94	980585.50	-44.61
651577.05	5019415.76	346	62.698	-39.11	980588.81	-46.13
652220.99	5019721.89	347	87.171	-35.82	980584.79	-45.58
652791.43	5020162.18	348	108.689	-33.05	980581.27	-45.21
653310.82	5020490.28	349	131.649	-29.66	980577.83	-44.39
654100.44	5020610.00	350	108.099	-30.85	980583.99	-42.95
654958.58	5020659.25	351	119.723	-29.11	980582.17	-42.50
655818.63	5020811.79	352	140.140	-26.68	980578.40	-42.36
653078.53	5020806.80	353	170.747	-26.49	980569.20	-45.60
652765.73	5021123.97	354	197.980	-24.63	980562.91	-46.79
652319.82	5021531.00	355	201.202	-24.44	980562.45	-46.96
650858.55	5019646.44	356	55.197	-38.60	980591.85	-44.77
650070.11	5019297.77	357	75.852	-34.31	980589.49	-42.79
637360.34	5018683.95	358	160.968	-18.03	980579.24	-36.04
637620.59	5018185.94	359	119.850	-23.31	980586.24	-36.72
638458.71	5018495.50	360	119.985	-24.73	980585.02	-38.15

639222.95	5018804.41	361	128.754	-25.18	980582.10	-39.59
640015.62	5018881.90	362	167.770	-22.04	980573.24	-40.81
640837.55	5018784.75	363	150.424	-25.78	980574.76	-42.62
641631.12	5019039.39	364	168.412	-22.67	980572.52	-41.51
642374.72	5019226.09	365	158.731	-20.47	980577.84	-38.23
642790.98	5018620.02	366	140.931	-19.17	980584.13	-34.94
642959.54	5017909.63	367	147.396	-16.72	980584.01	-33.21
643160.10	5017124.12	368	128.250	-17.08	980588.91	-31.43
643372.45	5016241.14	369	96.412	-18.66	980596.43	-29.45
643572.27	5015450.68	370	84.637	-19.05	980599.03	-28.52
643929.72	5016497.63	371	94.382	-18.75	980597.16	-29.32
644709.64	5016670.63	372	79.692	-21.14	980599.43	-30.06
645512.44	5016876.49	373	68.502	-23.54	980600.64	-31.20
646357.62	5017072.31	374	90.050	-23.03	980594.65	-33.10
647177.82	5017263.43	375	99.111	-24.10	980590.92	-35.19
647436.15	5017837.90	376	95.533	-25.15	980591.44	-35.84
648135.71	5018241.18	377	84.190	-28.43	980591.98	-37.85
648773.56	5018661.68	378	87.924	-29.72	980589.86	-39.56
649477.87	5019079.91	379	88.859	-31.03	980588.59	-40.97
649542.11	5022847.65	380	67.035	-34.34	980595.08	-41.84
648793.59	5023324.12	381	98.567	-30.56	980589.53	-41.59
647957.74	5023832.54	382	112.768	-29.26	980586.88	-41.88
647276.06	5024128.35	383	138.860	-26.27	980582.07	-41.81
646498.20	5023881.58	384	163.936	-23.11	980577.31	-41.45
645634.54	5023539.43	385	189.928	-19.68	980572.46	-40.93
644842.29	5023323.14	386	196.020	-18.85	980571.24	-40.79
644022.54	5023101.09	387	137.523	-25.33	980582.65	-40.72
643199.10	5022885.50	388	171.829	-21.09	980576.15	-40.31
642689.12	5023314.95	389	172.633	-20.37	980576.97	-39.69
642400.75	5022674.65	390	186.865	-19.29	980573.15	-40.20
641654.37	5022477.33	391	164.626	-21.05	980578.11	-39.47
641134.20	5022004.91	392	179.260	-18.99	980575.27	-39.05
641320.42	5021243.71	393	170.487	-21.34	980575.01	-40.42
641938.23	5021403.70	394	190.564	-20.99	980569.28	-42.31
641393.50	5020354.28	395	159.386	-25.01	980574.03	-42.85
640396.70	5020079.50	396	178.920	-19.68	980573.13	-39.70
639779.85	5019401.69	397	178.917	-19.31	980572.97	-39.33
636917.79	5017973.65	398	105.269	-24.42	980589.46	-36.20
636496.61	5018348.48	399	108.475	-23.71	980589.51	-35.84
636685.34	5019148.77	400	107.214	-23.52	980590.73	-35.52
636995.67	5019865.85	401	103.632	-23.77	980592.16	-35.37
637741.74	5020692.62	402	102.740	-23.73	980593.14	-35.22
640659.68	5023718.19	403	124.562	-22.51	980590.04	-36.45
640911.72	5022882.63	404	148.408	-21.18	980583.32	-37.79
640141.81	5025437.15	405	108.837	-21.33	980597.48	-33.51
639604.09	5026160.78	406	106.660	-19.89	980600.18	-31.83
634438.96	5021969.55	407	115.119	-18.98	980595.17	-31.86
634338.34	5021133.65	408	115.205	-19.52	980593.91	-32.42
634410.83	5020200.81	409	108.077	-21.35	980593.53	-33.44
634491.82	5019314.20	410	105.594	-22.54	980592.38	-34.36
634553.63	5018504.48	411	98.528	-24.40	980592.04	-35.43
634745.16	5017627.07	412	137.204	-21.51	980582.28	-36.86

634962.04	5016821.71	413	112.015	-24.59	980586.31	-37.13
635714.01	5017104.06	414	95.754	-26.41	980589.73	-37.12
636094.43	5017840.53	415	99.924	-24.88	980590.56	-36.06
636266.76	5017092.51	416	105.469	-25.03	980588.09	-36.83
637081.23	5019065.06	417	127.792	-21.17	980586.66	-35.47
637347.76	5017385.14	418	164.823	-19.29	980575.74	-37.73
636977.06	5016663.70	419	145.904	-21.49	980578.79	-37.81
636714.56	5015950.20	420	154.326	-20.28	980576.82	-37.55
636897.51	5015205.40	421	149.789	-20.34	980577.56	-37.10
637306.81	5014855.26	422	155.680	-19.58	980576.21	-37.00
637686.10	5014967.95	423	137.764	-21.91	980579.49	-37.33
638087.54	5015067.45	424	127.061	-23.85	980580.93	-38.07
638539.27	5015195.26	425	121.867	-25.54	980580.93	-39.18
638853.20	5014762.31	426	128.564	-26.00	980578.05	-40.39
637126.28	5014334.16	427	150.425	-19.43	980577.56	-36.26
637586.45	5013683.17	428	138.987	-20.26	980579.71	-35.82
638030.52	5013325.64	429	132.510	-21.16	980580.52	-35.99
638444.21	5013450.18	430	120.011	-23.44	980582.19	-36.87
637921.18	5012765.43	431	146.763	-18.24	980578.59	-34.66
638528.67	5012314.28	432	153.191	-17.34	980577.12	-34.48
638924.04	5011698.32	433	138.474	-16.27	980582.23	-31.76
638905.77	5011045.07	434	117.218	-15.91	980588.61	-29.03
635723.66	5007323.14	435	15.688	-13.93	980618.95	-15.68
635540.78	5008111.56	436	47.437	-12.26	980611.46	-17.57
635245.43	5008943.22	437	35.744	-16.73	980611.29	-20.73
634991.36	5009724.34	438	49.246	-17.67	980606.83	-23.18
634779.56	5010506.97	439	53.379	-21.81	980602.04	-27.79
634586.23	5011323.92	440	65.908	-23.53	980597.13	-30.90
634399.11	5012153.17	441	112.994	-20.91	980585.90	-33.55
634196.25	5013026.15	442	130.240	-20.50	980581.70	-35.08
633993.40	5013856.75	443	109.988	-23.77	980585.36	-36.07
633806.31	5014636.07	444	131.169	-22.66	980580.58	-37.33
633971.33	5015384.70	445	124.692	-24.44	980581.40	-38.39
634657.76	5015970.96	446	115.557	-24.97	980584.15	-37.90

Appendix II: Potential Field Model Descriptions and Models (lines 1-10)

Line 1: A north-looking longitudinal line. Excellent fit occurs between the observed and calculated gravity profiles; however, some discrepancies exist in the magnetic data that are attributed primarily to the orientation of the section with respect to the strike of local geology. The section between L5 and L6 is essentially parallel to strike and may be underlain by a small westward extension of the East Branch Brook gabbro (EB) cutting the line at an oblique angle. A cross section (line 6) through the area supports this interpretation.

Line 2: A north-looking longitudinal line. Excellent fit occurs between the observed and calculated gravity profiles; however, some discrepancies exist in the magnetic data that are attributed primarily to the orientation of the section with respect to the strike of local geology. The Pleasant Ridge (PR) and Beech Hill-True Hill (BH-TH) plutons intersect the line at oblique angle, which results in a large sectional width. "A" refers to the location of Anomaly A in the Clarence Stream deposit (see Figure 1).

Line 3: A north-looking longitudinal line. Excellent fit occurs between the observed and calculated gravity profiles; however, some discrepancies exist in the magnetic data that are attributed primarily to the orientation of the section with respect to the strike of local geology. The Sorrel Ridge Granite (SR) occurs as a small cupola to the G2 granite. Both units have similar physical properties; however, map patterns suggest that the Sorrel Ridge Granite extends this far north. The Pleasant Ridge (PR) and Beech Hill-True Hill (BH-TH) plutons intersect the line at an oblique angle, which results in a large sectional width. The peculiar shape of the Pleasant Ridge Granite near L7 is also interpreted to be a feature related to the oblique angle between geological strike and line orientation.

Line 4: A west-looking cross-section. Excellent fit occurs between the observed and calculated gravity profiles; however, some discrepancies exist in the magnetic data. A discrepancy occurs over the Tower Hill Granite (TH) for unknown reasons. Because samples for this study were collected from drill core from holes along the periphery of the intrusion, there may be lithological and susceptibility variations throughout the pluton.

Line 5: A west-looking cross-section. Excellent fit occurs between the observed and calculated gravity profiles; however, some discrepancies exist in the magnetic data, which may be associated with mafic bodies off-section (e.g. 17000-21000 m) and a small DC shift.

Line 6: A west-looking cross-section. Excellent fit occurs between the observed and calculated gravity profiles; however, some discrepancies exist in the magnetic data that are associated with a small DC shift and the limited strike of the Sorrel Ridge granite (SR). A small mafic body next to L1 represents the East Branch Brook gabbro (EB), as discussed in the description of Line 1.

Line 7: A west-looking cross-section. Excellent fit occurs between the observed and calculated gravity and magnetic profiles; however, some minor discrepancies in the magnetic data are related to deep long-wavelength source geometry. The Pleasant Ridge Granite (PR) can be seen to have a similar shape near the intersection of L7 and L3.

Line 8: A west-looking cross-section. Excellent fit occurs between the observed and calculated gravity and magnetic profiles. This line demonstrates the repetition and symmetry of magnetic responses imaged in the magnetic map patterns. The large east-west fault highlighted in the horizontal gradient data is shown at 21500 m, with displacement on the order of several thousand metres.

Line 9: A west-looking cross-section. Excellent fit occurs between the observed and calculated gravity and magnetic profiles. The Magaguadavic Granite (Ma) was not sub-divided as in line 9 in order to demonstrate the bulk response related to overall pluton geometry. The large east-west fault highlighted in the horizontal gradient data is shown at 21000 m, with displacement on the order of several thousand metres. The intersection of the Sawyer Brook Fault (SBF) with Line 9 is shown as a discrete magnetic low cutting the response from the Magaguadavic Granite (Ma). This low is interpreted to be indicative of fluid migration along the fault related to the emplacement of G2, as discussed in the text.

Line 10: A west-looking cross-section. Excellent fit occurs between the observed and calculated gravity profiles; however, some discrepancies exist in the magnetic data, in particular from 11000 to 15000 m. They are due to the fact that this portion of the model is exactly coincident with a northwest-trending fault and as discussed in the text, these faults are commonly characterized by magnetic lows. Hence the measured response is dramatically lower than the calculated response which reflects the typical magnetic effect of the surrounding (unaltered) Magaguadavic Granite (Ma). The John Lee Brook Granite (JLB) has essentially zero strike to the east (into page) and the small inclusion of Magaguadavic granite corresponds with mapped exposures east of this section. The BH-TH and G2 bodies also have essentially no strike into the page and the Mount Pleasant Porphyry is modeled adjacent to the section (east or into the page).

Legend for Potential Field Models (Lines 1-10)

STRATIFIED ROCKS

- Little Mount Pleasant Formation (LMP)
- Flume Ridge Formation (FR)
- Saint Croix terrane (SC, SC-u)
- Mascarene terrane (MT)
- New River terrane (NR)
- Sawyer Brook Fault (SBF)

INTRUSIVE ROCKS

- Bocabec Gabbro (BG)
- Tower Hill Granite (TH)
- Magaguadavic Granite (Ma)
- East Branch Brook Gabbro (EB)
- John Lee Brook Granite (JLB)
- G1 Granite (G1)
- G2 Granite (G2)
- Sorrel Ridge Granite (SR)
- Kedron Pluton (Ke)
- Pleasant Ridge Granite (PR)
- Beech Hill - True Hill Granite (BH-TH)
- McDougall Brook Microgranite (MB)

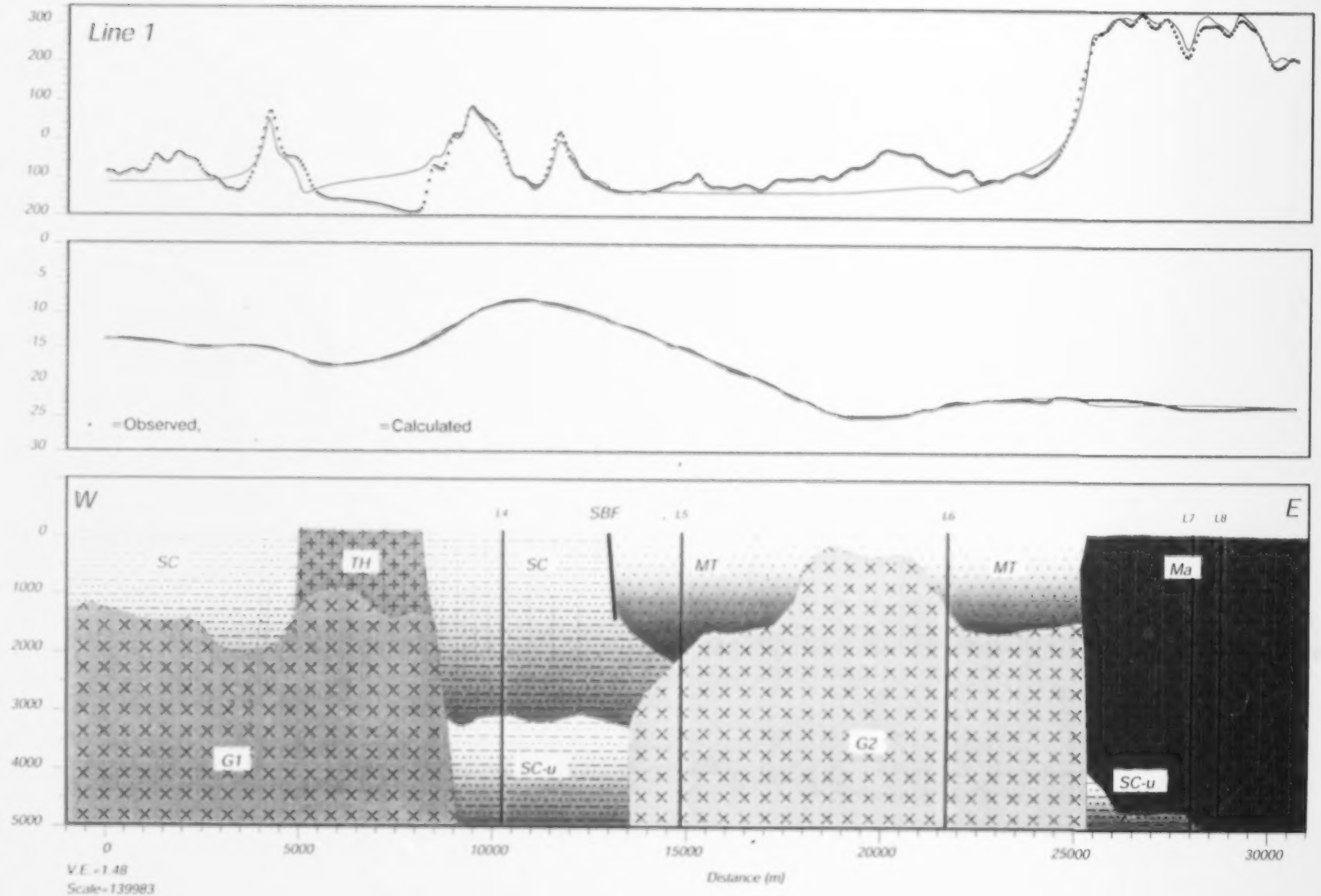
Line 1
Magnetics (nT)
300
200
100
0
100
200
Gravity (mGal)
0
5
10
15
20
25
30
=Observed,
=Calculated
W
E
Depth (m)
0
1000
2000
3000
4000
5000
L4
SBF
L5
L6
L7
L8
SC
TH
SC
MT
MT
Ma
G1
SC-u
G2
SC-u
0
5000
10000
15000
20000
25000
30000
V.E.=1.48
Scale=139983
Distance (m)

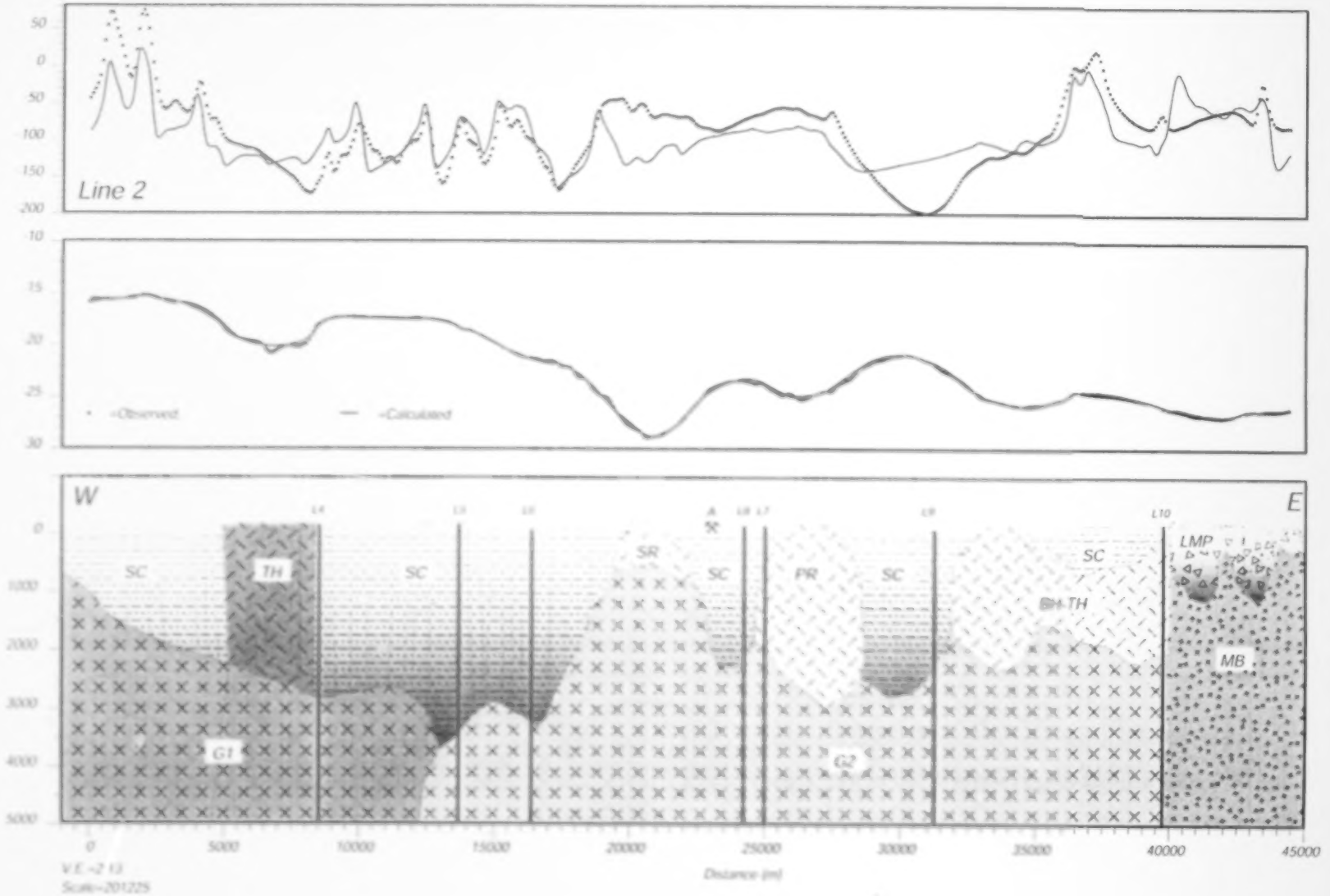
Magnetics (nT)
50
0
-50
-100
-150
-200
Line 2
Gravity (mGal)
10
15
20
25
30
•=Observed
—=Calculated
W
E
Depth (m)
0
1000
2000
3000
4000
5000
L4
L3
L5
A
L8
L7
L9
L10
SC
TH
SC
SR
SC
FR
SC
SC
TH
LMP
MB
G1
G2
0
5000
10000
15000
20000
25000
30000
35000
40000
45000
V.E.=2 (3
Scale=1:20225
Distance (m)

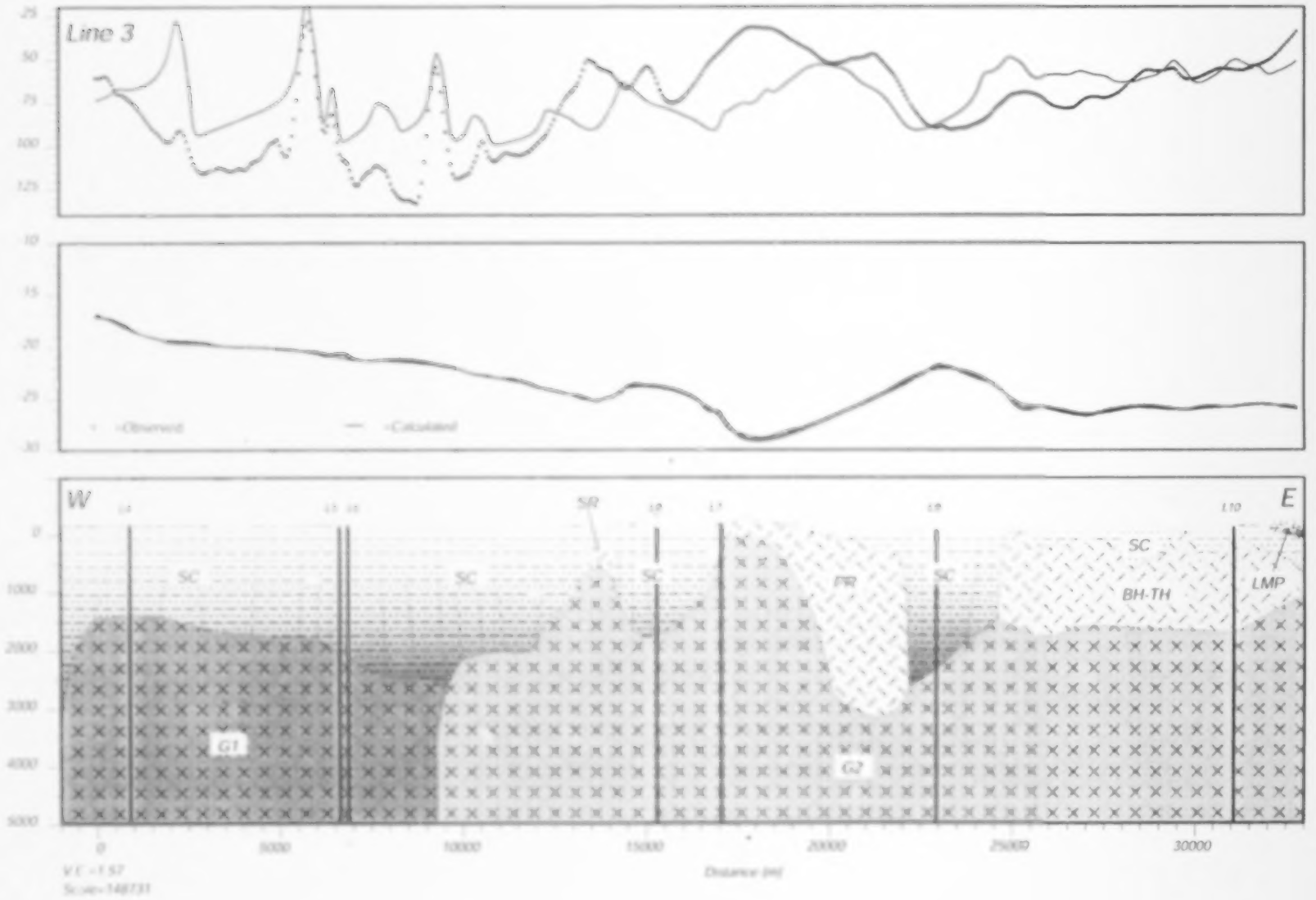
Line 3
Magnetics (nT)
Gravity (mGal)
Observed
Calculated
W
E
SC
SR
FR
BH-TH
LMP
G1
G2
Depth (m)
Distance (m)
V.E. =1.57
Scale=1:48731

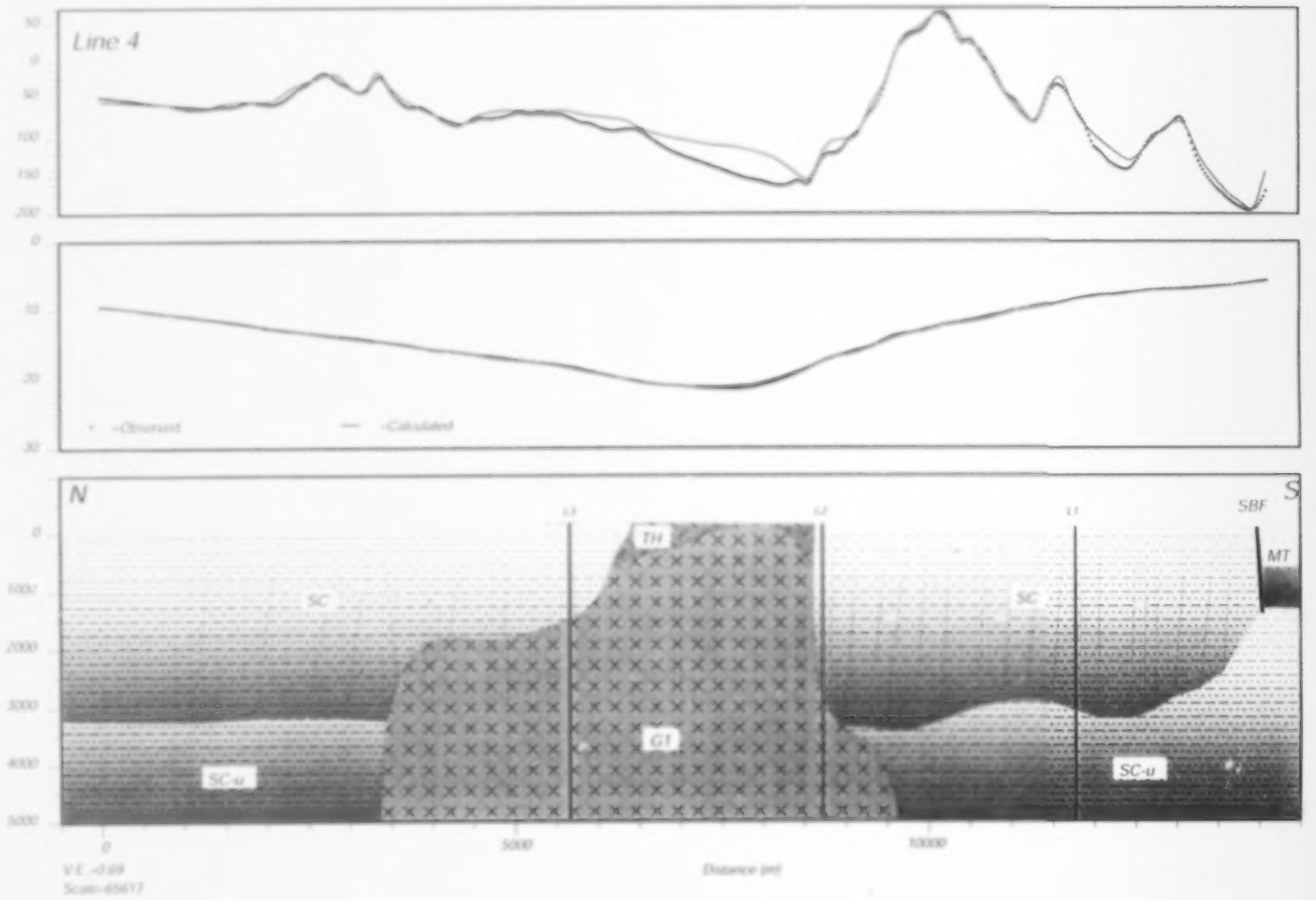
Line 4
Magnetics (nT)
50
0
-50
-100
-150
-200
Gravity (mGal)
0
10
20
30
-Observed
-Calculated
Depth (m)
N
S
SBF
MT
TH
G1
SC
SC-u
L1
L2
L1
0
1000
2000
3000
4000
5000
0
5000
10000
V.E.=0.69
Scale=1/56617
Distance (m)

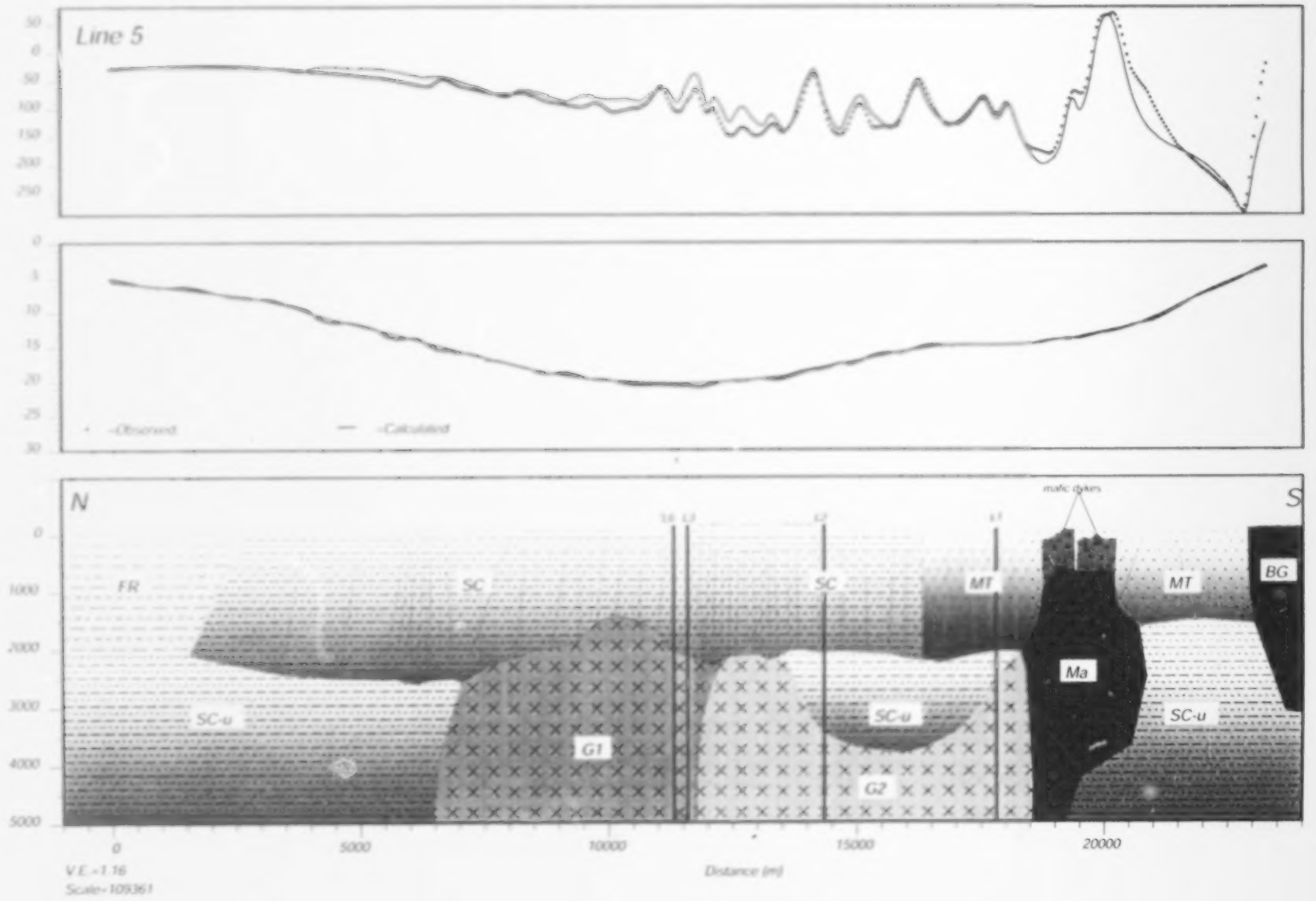
Line 5
Magnetics (nT)
50
0
-50
-100
-150
-200
-250
Gravity (mGal)
0
-5
-10
-15
-20
-25
-30
-Observed
-Calculated
Depth (m)
N
S
0
1000
2000
3000
4000
5000
FR
SC
SC
MT
MT
BG
Ma
SC-u
SC-u
SC-u
G1
G2
mafic dykes
0
5000
10000
15000
20000
Distance (m)
V.E.=1.16
Scale=109361

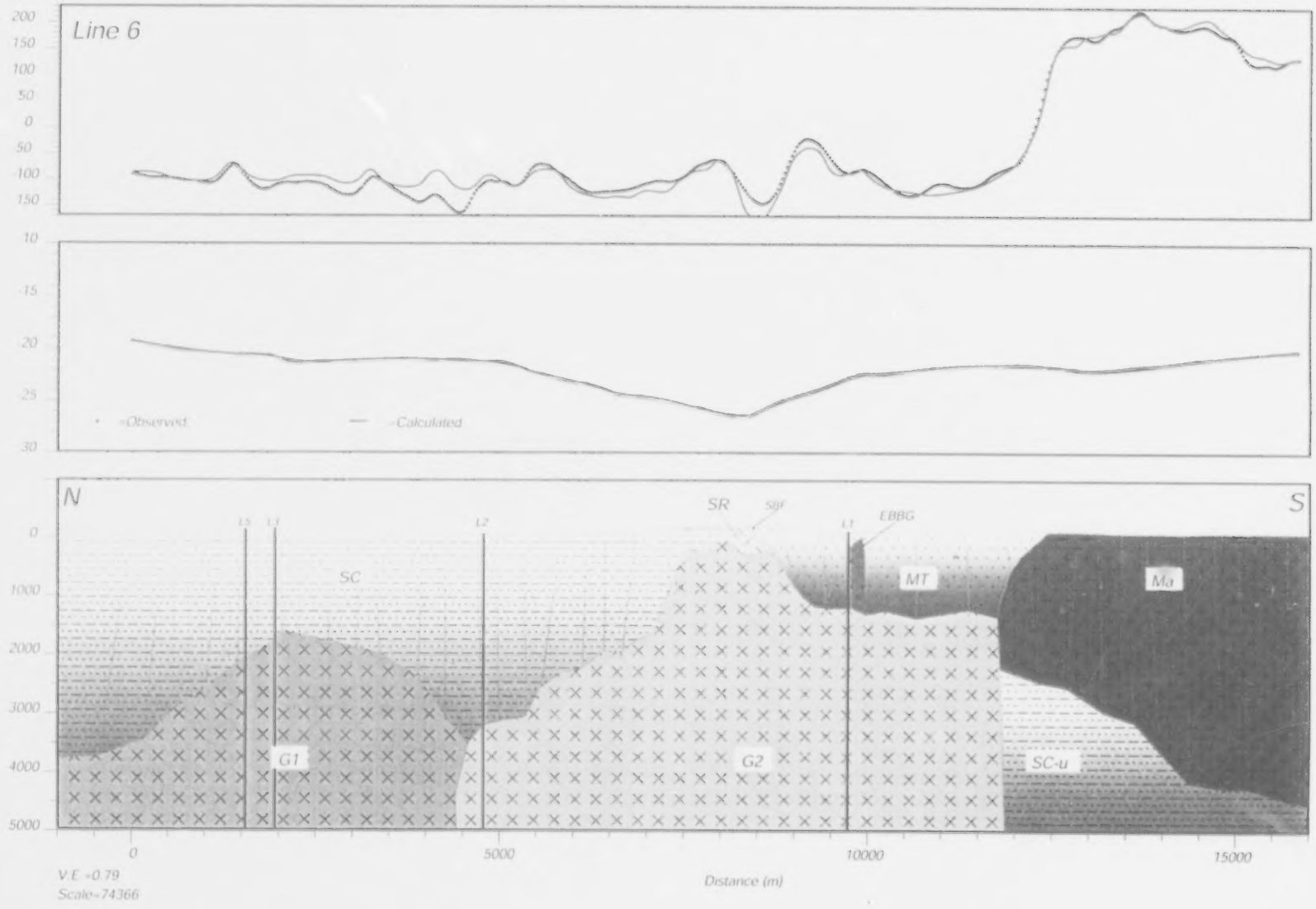
Line 6
Magnetics (nT)
200
150
100
50
0
50
100
150
Gravity (mGal)
10
15
20
25
30
·=Observed
—=Calculated
N
S
SR
SBF
EBBG
L5
L3
L2
L1
SC
MT
Ma
G1
G2
SC-u
Depth (m)
0
1000
2000
3000
4000
5000
0
5000
10000
15000
V.E.=0.79
Scale=74366
Distance (m)

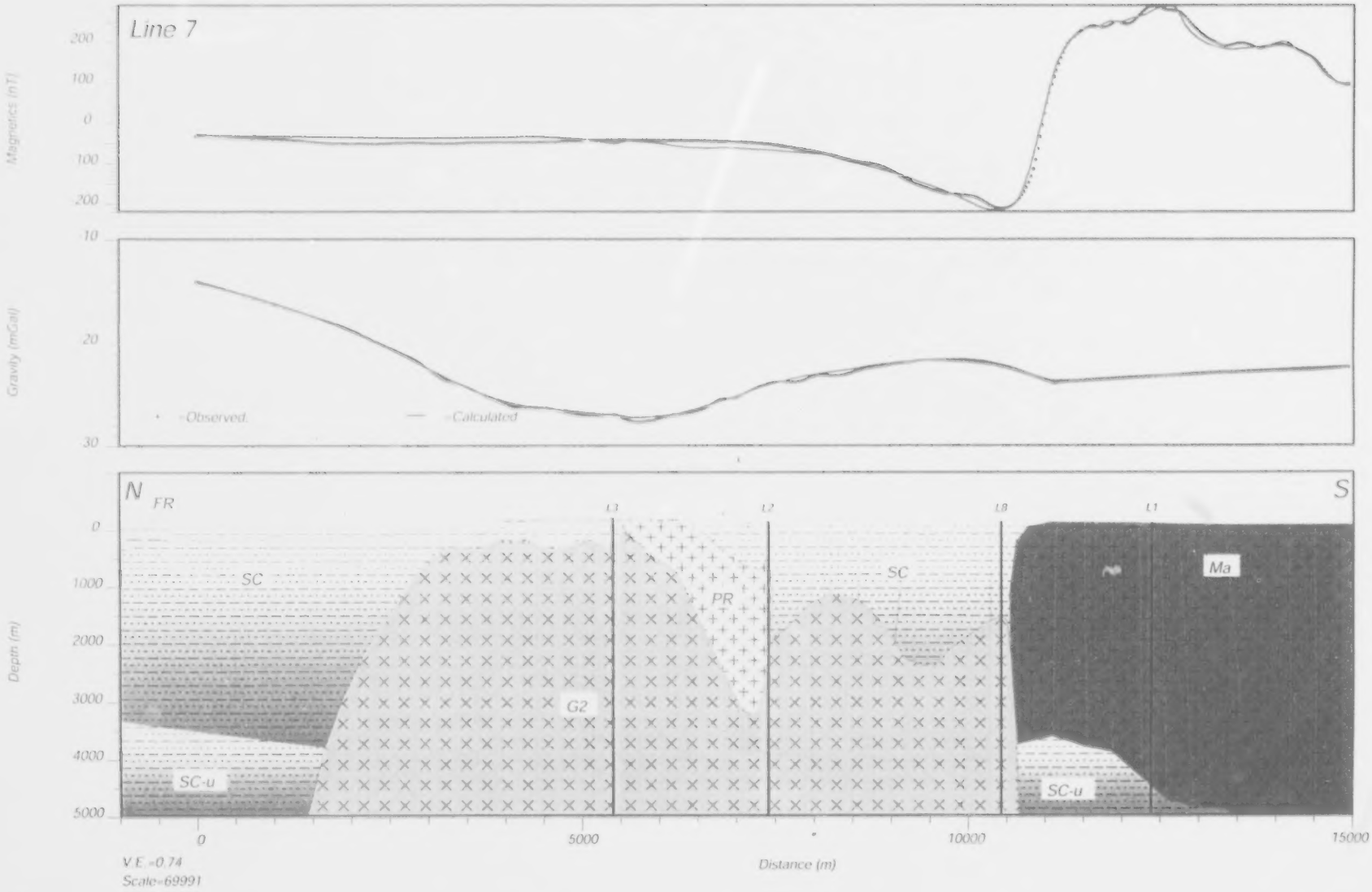
Line 7
Magnetics (nT)
200
100
0
100
200
Gravity (mGal)
10
20
30
+=Observed.
—=Calculated
N
FR
S
L3
L2
L8
L1
Depth (m)
0
1000
2000
3000
4000
5000
SC
PR
G2
SC-u
SC
Ma
SC-u
0
5000
10000
15000
V.E.=0.74
Scale=69991
Distance (m)

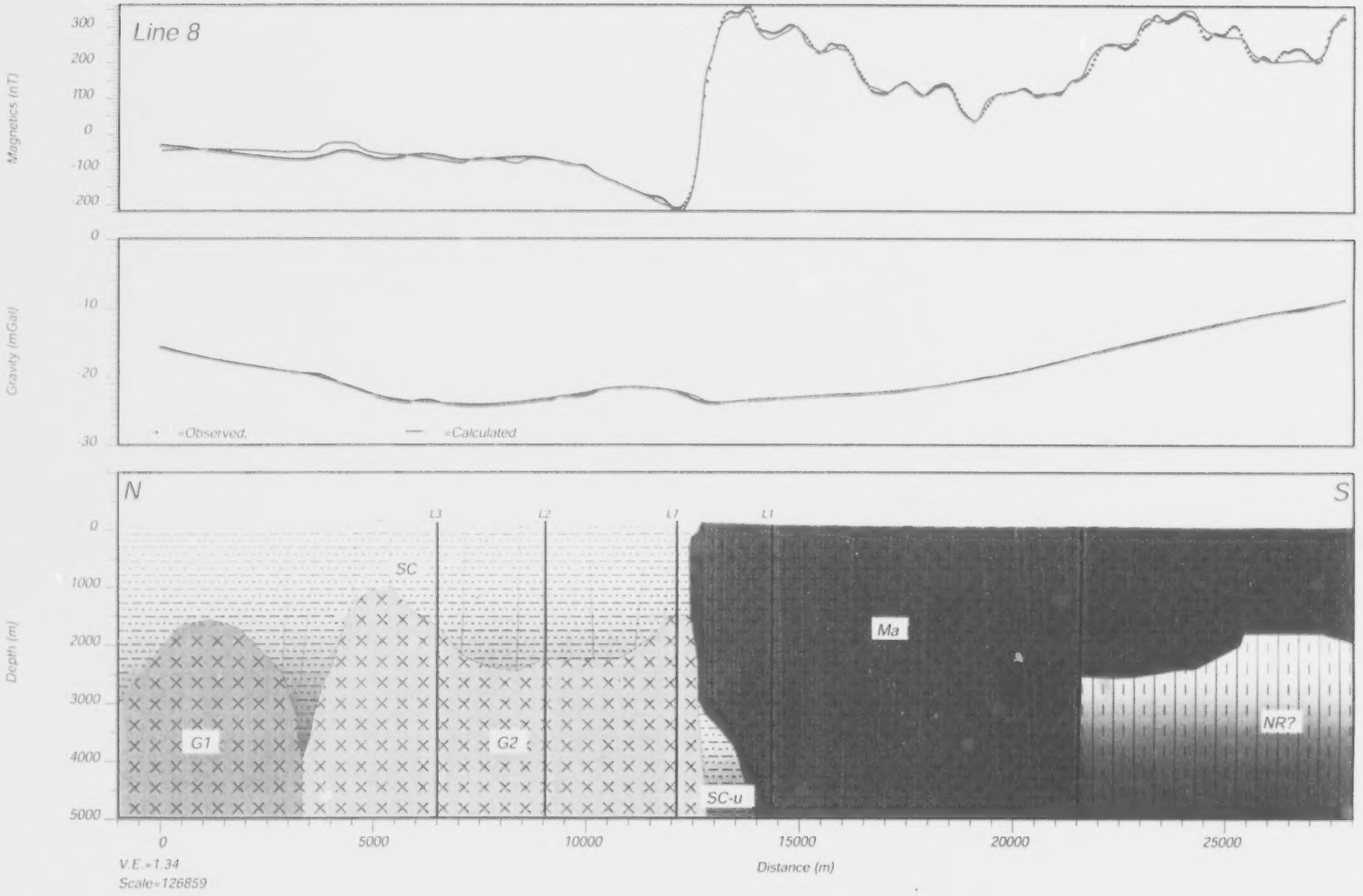
Line 8
Magnetics (nT)
300
200
100
0
-100
-200
Gravity (mGal)
0
-10
-20
-30
=Observed,
=Calculated
N
S
L3
L2
L1
SC
G1
G2
Ma
NR?
SC-u
Depth (m)
0
1000
2000
3000
4000
5000
0
5000
10000
15000
20000
25000
V.E.=1.34
Scale=126859
Distance (m)

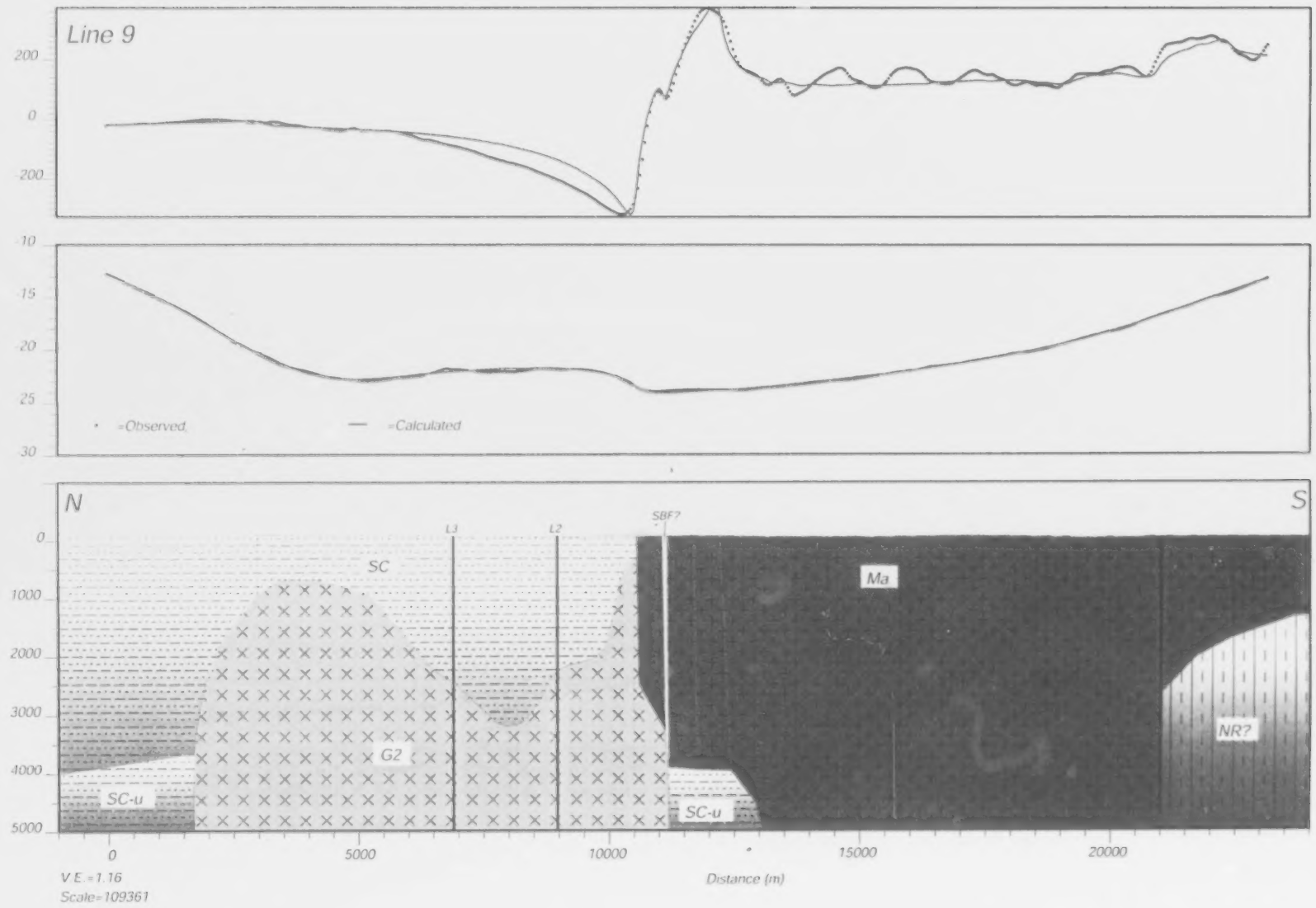
Line 9
Magnetics (nT)
200
0
-200
Gravity (mGal)
-10
-15
-20
-25
-30
=Observed
=Calculated
N
S
Depth (m)
0
1000
2000
3000
4000
5000
L3
L2
SBF?
SC
Ma
G2
NR?
SC-u
SC-u
0
5000
10000
15000
20000
V.E.=1.16
Scale=109361
Distance (m)

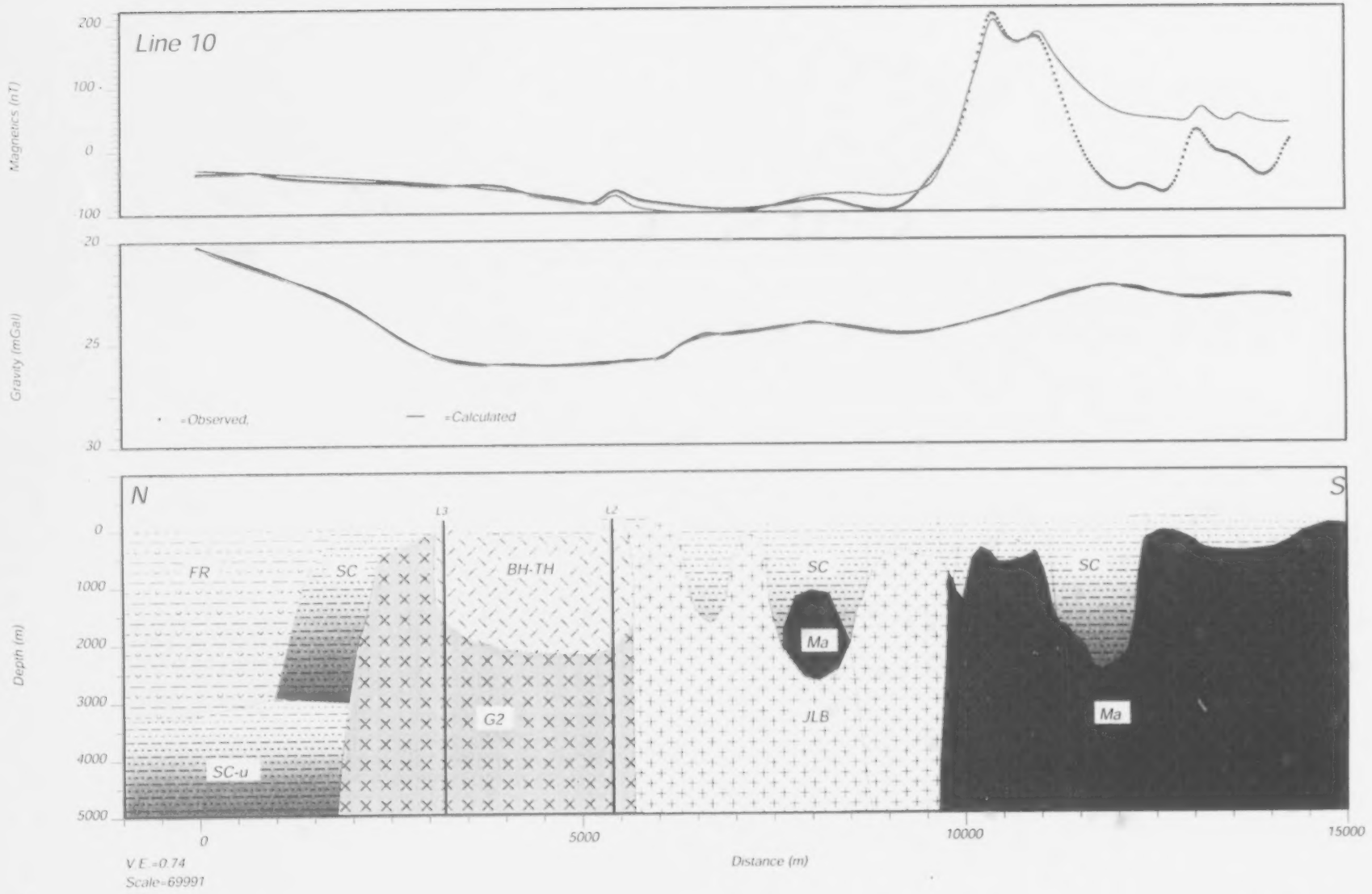
Line 10
Magnetics (nT)
200
100
0
100
Gravity (mGal)
20
25
30
• =Observed,
— =Calculated
N
S
L3
L2
Depth (m)
0
1000
2000
3000
4000
5000
FR
SC
BH-TH
SC
SC
Ma
Ma
G2
JLB
SC-u
0
5000
10000
15000
Distance (m)
V.E.=0.74
Scale=69991